RRS *Charles Darwin* Cruise CD 99

Cruise Report

Near-bottom geophysical studies of the Broken Spur spreading segment, Mid-Atlantic Ridge 29°N

Lisbon, Portugal to Ponta Delgada, Azores
3 March - 9 April 1996

Department of Geological Sciences,
University of Durham,
Durham, DH1 3LE, UK

April, 1996

RRS *Charles Darwin* Cruise CD 99

Lisbon, Portugal to Ponta Delgada, Azores
3 March - 9 April 1996

Near-bottom geophysical studies of the Broken Spur spreading segment, Mid-Atlantic Ridge 29°N

R. C. Searle[1] and the shipboard scientific party[2]

Department of Geological Sciences,
University of Durham,
Durham, DH1 3LE, UK

April, 1996

---

[1] University of Durham, Chief Scientist

[2] N. C. Mitchell, J. Escartin, P. Slootweg, S. Russell (University of Durham),
P. Cowie, S. Allerton (University of Edinburgh),
C. J. MacLeod (University of Wales, Cardiff),
T. Tanaka (University of Chiba, Japan),
C. Flewellen, I. Rouse, D. Edge (Southampton Oceanography Centre, Ocean Technology Division),
D. Booth, C. Day, A. Fern, G. Knight, P. Mason, D. Teare (Research Vessel Services)

Table of Contents

Frontispiece (opposite): Left, TOBI swath bathymetry over part of the western valley wall fault; range (1-1500 m) vs. ping number (1-1000). Right, Simrad EM12 bathymetry from the same area. Depths in metres; contour interval 20 m. (The TOBI data have not been fully geographically registered). This and some other images in this report were produced using GMT software (Wessel & Smith, 1991, 1995).

Background and objectives

(Roger Searle, based on NERC grant proposal)

Mid-ocean ridge spreading centres are divided into discrete segments about 50 km long, where new lithosphere is created and extended by magmatic (volcanic) and tectonic (faulting) processes. *Our primary objective on this cruise, which was funded by BRIDGE, was to quantify the contribution of fault strain to plate separation along a single segment* of the Mid-Atlantic Ridge near 29°N, 43°W ('Broken Spur' segment). This segment was chosen because it has a clearly-defined structure, good existing data coverage extending out to the ridge flanks, and was becoming a focus for international studies.

We intended to use data primarily from TOBI's sidescan, swath bathymetry, and three-component magnetometer to determine the displacements and dips of faults, degree of tilting of fault blocks, spacing of faults, etc. The new swath bathymetry and magnetometer on TOBI had been developed for just this purpose. The SIMRAD multibeam echo-sounder was to be used to make a detailed base map on which to locate TOBI.

We proposed to obtain complete TOBI coverage out to a distance of 35 km from the axis. The survey would extend along strike from the 'magmatically robust' segment center to the 'magmatically starved' segment end, in order to look for variations in the amount of strain and faulting style over two dimensions.

We also planned to examine the inter-relationship between magmatism and tectonism, using the magnetic data to document the fine structure of the magma emplacement process. The use of three-component magnetics can reveal details of crustal structure (e.g. block rotations) not previously accessible with total-field measurements. The method had been developed for ship-board use by Japanese colleagues, but the use in a deep-towed instrument would be new.

We also intended to study sediment accumulation and mass wasting processes in the median valley walls, using an upgraded chirp profiler to be developed for TOBI, since these processes affect the measurement of strain. Finally, we were to use the new video imaging tool SHRIMP to ground-truth the TOBI data.

Prof. Joe Cann and Dr. Donna Blackman (University of Leeds) were running the cruise following ours, CD100. They would be carrying out somewhat similar studies on the next segment north, using an almost identical suite of equipment, so we liaised closely with them.

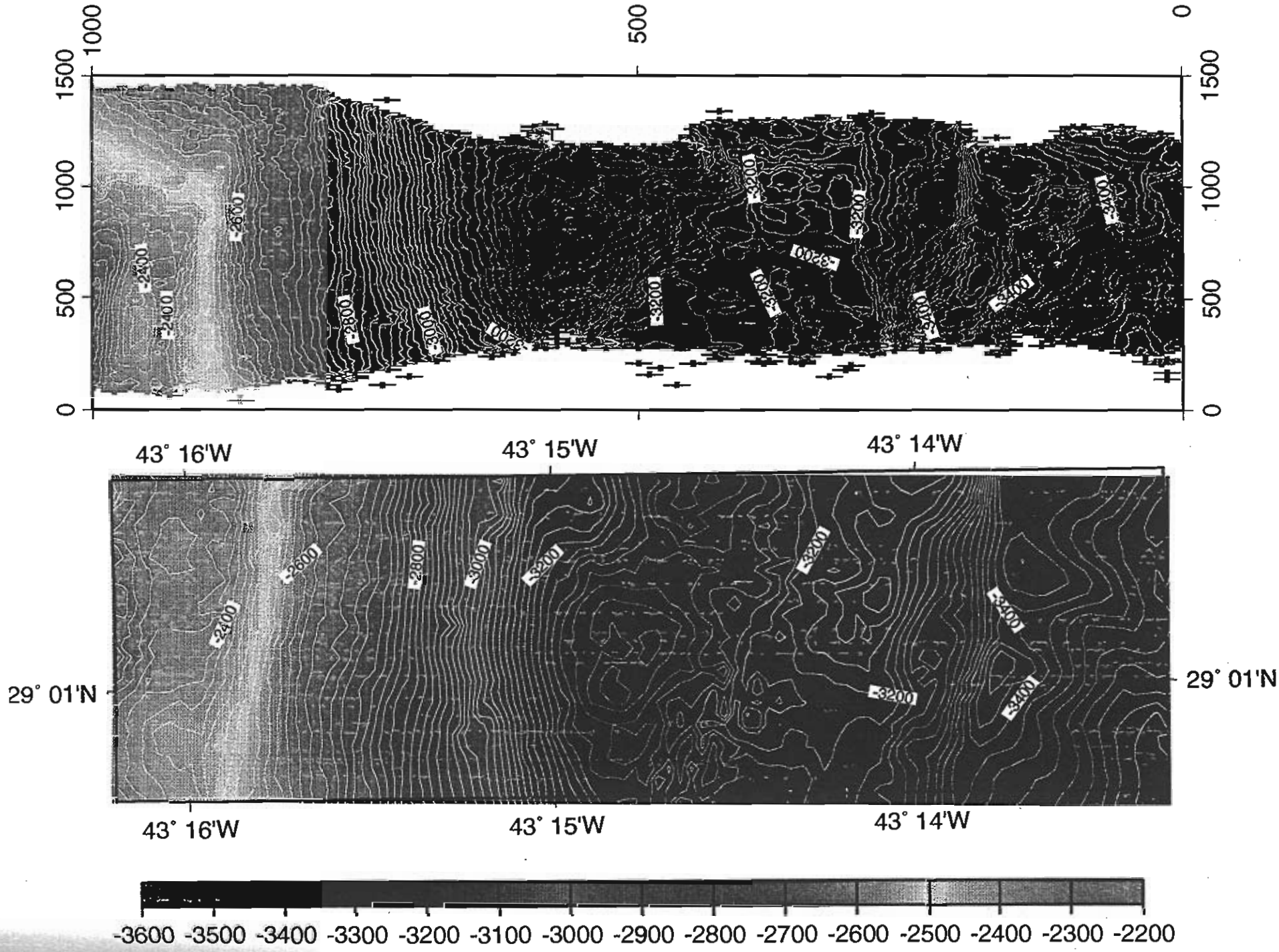
1000
500
0
1500
1000
500
0
-2400
-2600
-2800
-3000
-3200
-3400
43° 16'W
43° 15'W
43° 14'W
29° 01'N
-3600 -3500 -3400 -3300 -3200 -3100 -3000 -2900 -2800 -2700 -2600 -2500 -2400 -2300 -2200

Overview and summary

(Roger Searle)

On the previous cruise it had been discovered that the conducting tow-cable was damaged and needed replacing. Although a replacement was sent to Lisbon, it was late, causing a 36 hour delay in sailing.

On sailing, the new TOBI magnetometer was working, but the swath bathymetry was not, although we anticipated being able to get it to an operational state during the cruise.

Passage to the work area (Figure 1) provided the opportunity for a number of test dips for further work on TOBI, for tensioning the new tow-cable, and for calibrating the Simrad EM12 multibeam and the shipboard three-component magnetometer (STCM). The latter was done by steaming the ship in a figure of eight pattern.

Also on passage we planned our TOBI survey. We aimed for twenty east-west lines, 2 km apart and extending up to 35 km off-axis; those lines we achieved are shown in Figure 2. These lines were identified by letters A-T from north to south. We planned to run alternate ones initially to give an overall sidescan coverage then, time permitting, to interlace the others to give complete north-looking and south-looking sidescan coverage (and, we hoped, complete bathymetric coverage).

When we reached the survey area on March 12th, the TOBI bathymetry was still not working, so we provided the opportunity for further tests, carrying out dredge stations D1 - D3 and further STCM calibrations while we waited. The dredges were to investigate the rock types exposed on the major fault scarp at the southern Inside Corner High and to obtain material from the median valley floor for rock magnetisation studies. We also attempted some SHRIMP stations, but eventually the camera failed without having produced any usable results. In the absence of SHRIMP, we alternated dredging with some north-south EM12 survey lines. Ship tracks in the survey area are shown in Figure 3.

The first planned TOBI survey line (T) was started on March 14 with an expectation of some phase bathymetry. However, it was soon realised that the phase signal was severely clipped, so we recovered mid-way through the line.

Further STCM calibrations, dredge stations D4 - D5, and and a further EM12 survey occupied us until March 16 when TOBI was ready for another try. By this point we had decided to start running complete TOBI survey lines even without its bathymetry, in order to get some usable data for tectonic studies, and hope that further adjustments to the phase system could be carried out as we went along or at ends of lines. Lines G and I were thus run on March 16 - 18. They produced excellent sidescan but no useful bathymetry and, due to a minor error, they also failed to log any magnetics.

On the night of March 18 - 19 we ran the SHRIMP, with a pinger attached but no camera, to obtain two high-resolution bathymetry and shallow sub-bottom profiles over a fault scarp in the western crestal mountains.

TOBI was re-launched on the morning of March 19 at the start of line O, with operational sidescan and magnetometer, and an expectation of phase bathymetry to about half range on both sides, although by an oversight only the starboard side was connected. At the end of this line TOBI was recovered briefly and the port bathymetry connected. It was then redeployed, and lines M, Q, and S were run.

On March 23 there was a current surge in the tow-cable and TOBI stopped working and was recovered. This proved to be due to a short circuit in the depressor-weight's slip-rings; three more such faults occurred during the course of the cruise, but were repaired by recovering the depressor only, not TOBI.

Lines K, E, C, A, F, and part of J were then run before recovering TOBI on March 29 for routine maintenance. Two further dredges were attempted (D6 lost) before redeploying TOBI on March 30 for the remainder of line J, and lines H, L, N, and P. We then (April 3-4) ran two strike lines (U and V) on the west and east sides of the median valley to follow individual faults continuously from segment end to segment centre, before returning to part of line R, which was run until the final recovery and departure from the work area in the morning of April 5.

Of the twenty planned TOBI lines, we had completed all of sixteen (A, C, E - Q, and S), and parts of two more (R and T). Lines B and D were left, with an agreement that Cann would complete them during CD100.

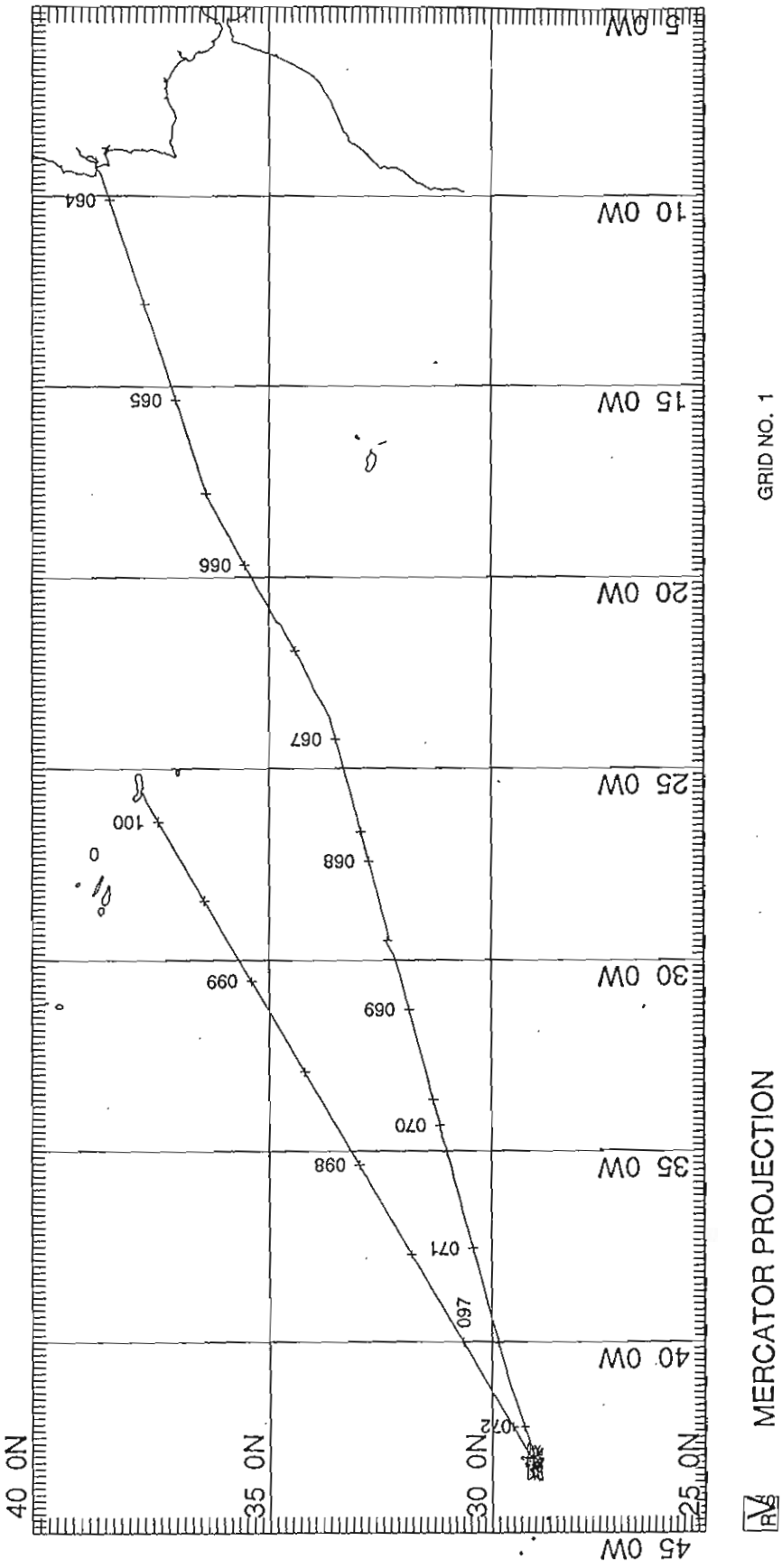

Figure 1: Overall track chart, cruise Charles Darwin CD99. Tick marks every 12 hours; annotated with Julian day number at 0000 hours.

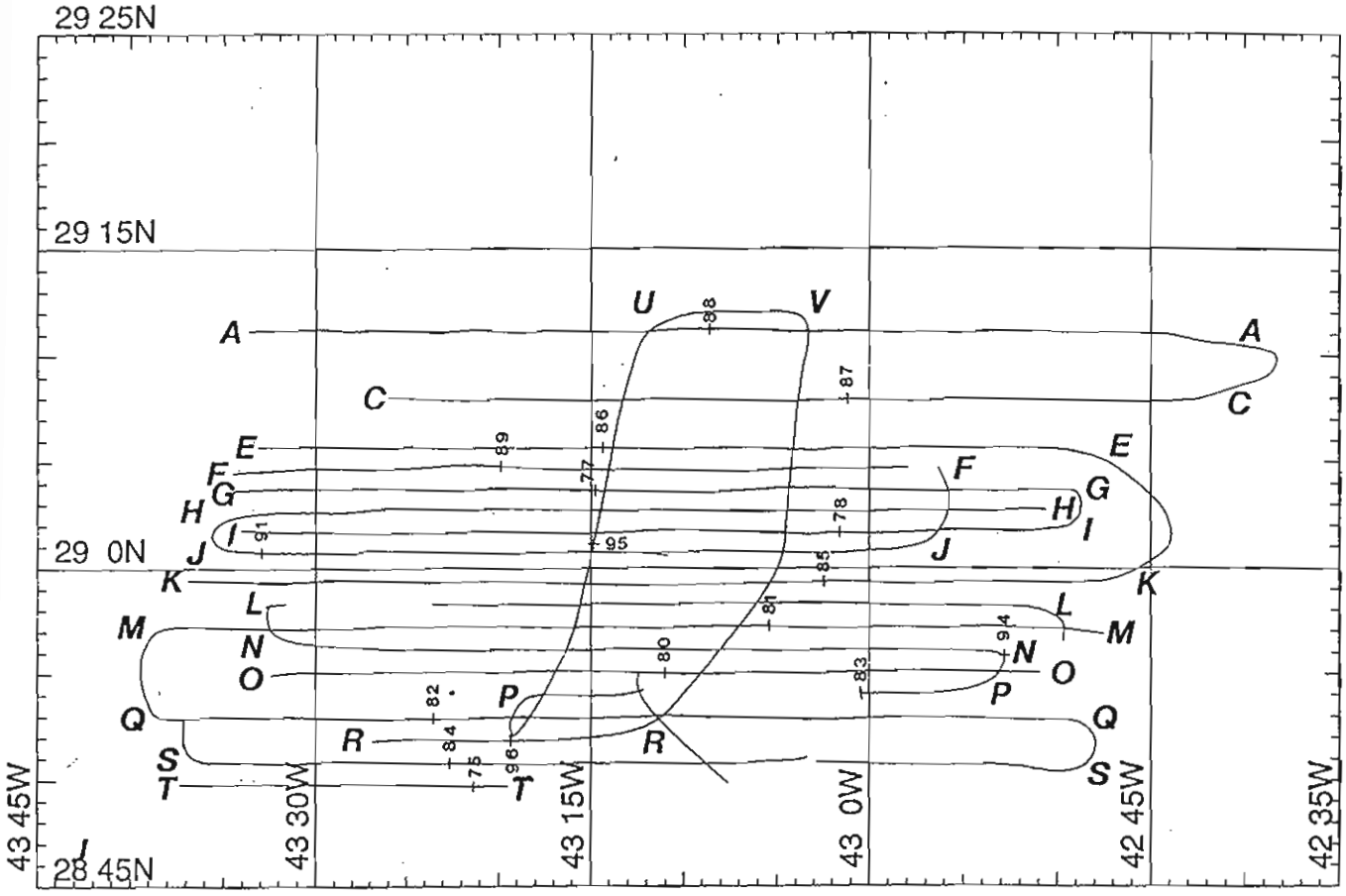

MERCATOR PROJECTION

GRID NO. 2

SCALE 1 TO 750000 (NATURAL SCALE AT LAT. 0)

INTERNATIONAL SPHEROID PROJECTED AT LATITUDE 0

CD99 Work Area Track Plot: **TOBI**. Day number at OO GMT

Figure 2: TOBI track in survey area (see text for navigation method). Tick marks annotated with Julian day number at 0000 hours.

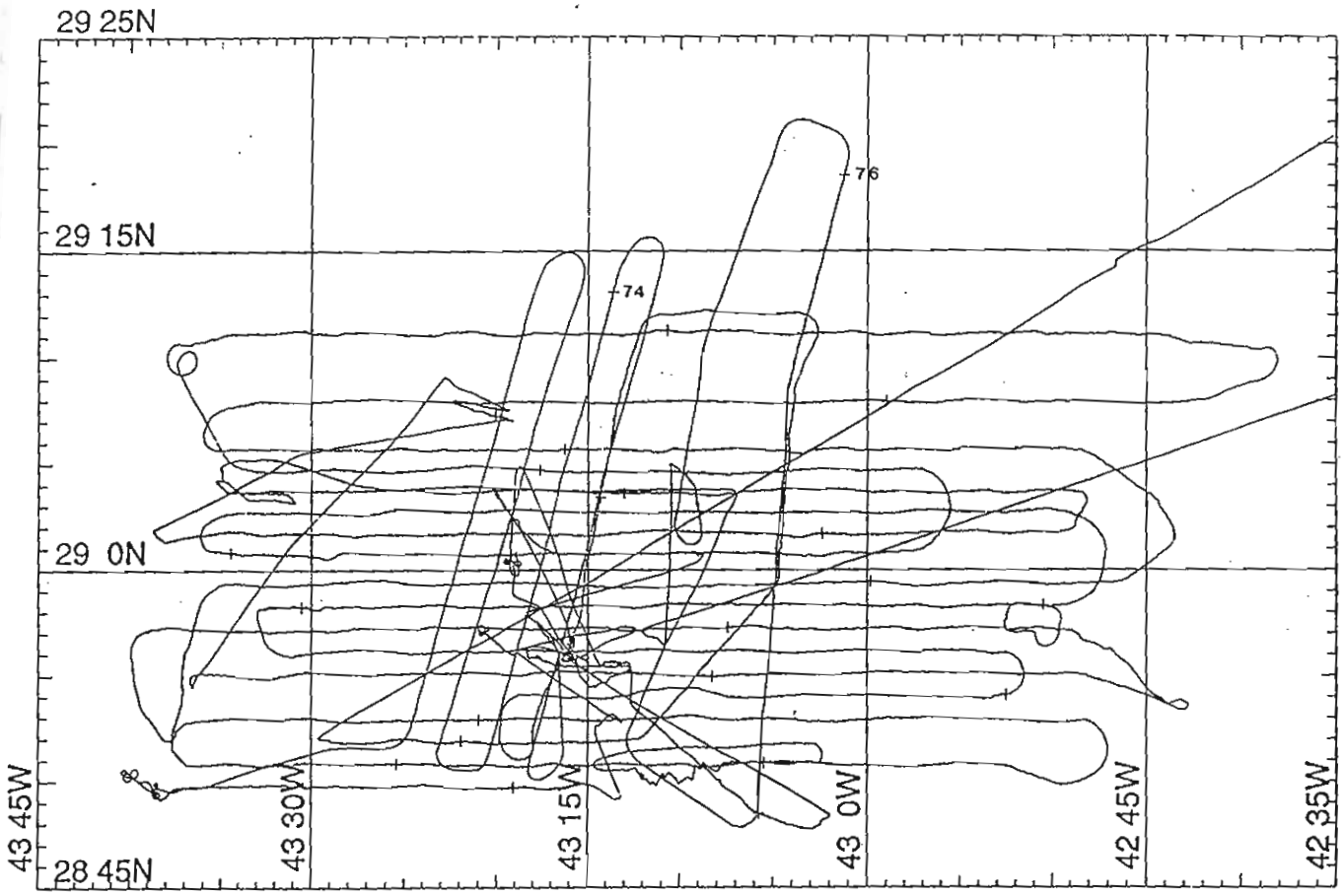

MERCATOR PROJECTION

GRID NO. 2

SCALE 1 TO 750000 (NATURAL SCALE AT LAT. 0)

INTERNATIONAL SPHEROID PROJECTED AT LATITUDE 0

CD99 Work Area Track Plot : Ship

Figure 3: Ship's track in survey area. Tick marks every 24 hours at 0000 hours.

Diary of events

(Roger Searle)

All times GMT (with Julian day number). A summary table of the operations is given on page 60.

1996, Friday March 1 (061)
Scientific party joined ship in Lisbon. Awaiting replacement conducting tow-cable to replace one found damaged on previous leg. Ship's agent reports cable's driver arrested at French/Spanish border by police.

Saturday March 2 (062)
Informed new driver on his way with cable.

Sunday March 3 (063)
0800: Cable arrives. Began loading onto ship 0900, then spooling onto Darwin's winch drum. Sailing delayed until enough weight transferred for stability.
1900: Depart Lisbon; set course WSW for science area, 11 knots.

Monday March 4 (064)
Weather fair, clear skies.
1548: Passed Waypoint 1 (37°30'N, 9°10'W), 200 mile limit. A/c 252°.
1600: Simrad EM12 switched on, running unmanned overnight.
Instituted series of daily seminars: today's on 'Segmentation' by Searle.

Tuesday March 5 (065)
0800: Heave to for velocimeter dip prior to EM12 calibration run. Wind NE 25 knots, moderate swell. Decided weather too poor for EM12 calibration, so aborted dip.
0906: Continue on passage.
1229: Waypoint 2 (36°20'N, 17°55'W). A/c 241°, avoiding Portuguese 200 mile limits.
1250: Deploy first expendable bathythermograph (XBT).
1400: Load test for tow-cable termination - OK. Seminar on 'Sediments' by Mitchell.
1500: Reduce speed to 3 then 6 knots; commence streaming tow-cable for tensioning.
2025: Cable tensioning completed.
Weather appeared to be moderating by late evening.

Wednesday March 6 (066)
Weather had worsened again overnight. Northerly wind of 30 knots all day prevented EM12 calibration or TOBI test. Continued on passage.
1400: Seminar on 'Ophiolites' by MacLeod and Allerton.
2112: WP 3 (33°40'N, 23°40'W). A/c 255°.

Thursday March 7 (067)
Continuing northerly wind of 35 knots in morning, gradually falling and pressure rising. 20 knot wind by evening but still heavy swell preventing TOBI deployment. Afternoon seminar by Russell, Tomoko and Allerton on Magnetics.
0902-0921: Conducted 'Figure-of-eight' manoeuvre to calibrate Shipboard Three Component Magnetometer (STCM), starting clockwise, turning at 36° per minute at 6-8 knots.
1316: XBT no. 1
1506: Hove to for velocimeter dip no. 1.
1800: Velocimeter dip finished; transferring sound velocity data to EM12.
1942: Manoeuvring to start of EM12 calibration.
2012: Begin EM12 calibration run, S/c 075°, 8 knots.
2117: Alter to reciprocal course.
2211: Begin reciprical run.
2314: EM12 calibration run completed; resume passage to science area.

Friday March 8 (068)
Weather much improved, light wind from N but still moderate swell.
0950: Heave to preparing for first TOBI test deployment.

1020: TOBI in water.
1111: Short circuit in TOBI cable: begin recovery.
1314: TOBI recovered.
1330: Resume passage.
Prime fault traced to plug on depressor weight, but short caused damage in vehicle needing repairs. Following this, routine check of umbilical cable revealed low insulation resistance, so replaced.
2100: Heave to for second TOBI trial.
2122: TOBI in water.
2153: A further short circuit: recovering TOBI. This short subsequently traced to worn connector on vehicle.
2220: Resumed passage.
Afternoon seminar by Escartin on Faulting at Slow Spreading Ridges.

Saturday March 9 (069)
Wind northerly 15 knots. Little swell.
Seminar by Cowie on fault dimensions, growth and populations.
1342: Hove to for third TOBI launch.
1404: TOBI in water and working!

Sunday March 10 (070)
0730: Preparing to recover TOBI.
0825: TOBI on board. TOBI swath still not working, but useful understanding acquired during run. Main problem now is that removal of noisy filter has caused pre-amp to overload and clip signal. Gains will be modified before trying again.
0842: Resume course 255°, deploy towed proton magnetometer prior to second STCM calibration.
0949-1044: Commence figure of eights for STCM starting clockwise: first at 40° /minute, second at 20°/minute.
1556: XBT no. 3.
Continuing good weather. Seminar by Slootweg on TOBI processing. Science meeting to plan station work and TOBI survey.

Monday March 11 (071)
Seminar by Russell on Iberia Margin and Edge on SHRIMP.
1542: Reduce speed, recover towed magnetometer, prior to TOBI launch.
1614: TOBI in water. Another short circuit!
1700: TOBI recovered. Fault finally traced to end of umbilical cable where it enters TOBI.
1715: XBT no. 4. S/c 255° for science area.
1900: Way point 4 revised to southern end of segment; a/c 251°.

Tuesday March 12 (072)
0510: Arrived science area at S end of Broken Spur segment.
0510-0738: Sound velocity dip no. 2 (28° 55'.9N, 43° 16'.0W).
0535: XBT 5.
0738: Manoeuvre to low field gradient area for figure-of eight (STCM).
0949-1025: Run figures of eight near 29° 01'N, 43° 19'W, this time running two complete '8's, first starting clockwise, second starting anticlockwise. Thus four complete circles, of which second and third are continuously antclockwise. This test showed a definite problem with the STCM gyro which logged < 360° for a complete circle.
1055-1147: S-N run along basin centred near 29° 02'N, 43° 19'W using hull-mounted echosounder, to search for possible sediment cover.
1305: Begin dredge station D1 at 28° 55'.4N, 43° 14'.2W.
1443: Dredge on bottom, s/c 090° 0.5 knot.
1511: Dredge off bottom.
1634: Dredge on board. Few small pieces of fairly fresh pillow rind.
1634: XBT 6 and 7 aborted.
1715: Deploying TOBI for trial run along trace of eastern non-transform offset at S end of segment.
2345: Port bathymetry signal died. Recovering TOBI.

Wednesday March 13 (073)
0226: TOBI on board. Had achieved half range bathymetry on starboard side, still not much on port.

0416: Hove to. SHRIMP launched at 28° 55'.9N, 43° 15'.9W (station S1) for run up median valley boundary fault.
0434: Pressure sensor not working. Deploy PES fish.
0620: Acoustic monitor failed. Hauling in.
0808: SHRIMP recovered.
0907-1343: Dredge station D2 at 28° 54.5'N, 43° 14.8'W over southern tip of neovolcanic ridge. Excellent haul of basalt. Still working on TOBI and SHRIMP.
1500-1842: Dredge station D3 at 28° 56.0° N, 43° 17.7'W, on upper part of southern end of western median valley bounding fault, above talus ramp. Good haul including basalt debris with slickensides, cataclasites, and fault breccia.
1617: XBT no. 10.
1915: TOBI and SHRIMP not expected on line until morning. Streaming magnetometer and commencing Simrad EM12 survey of innermost faults on western part of segment using strike-parallel lines. S/c 015°, 8 knots.
2021: A/c at S end of line 1.
2325: A/c at N end of line 1.
2350: A/c at N end of line 2.

Thursday March 14 (074)
Weather continues excellent.
0257: A/c at S end of line 2.
0325: A/c at S end of line 3.
0611: A/c at N end of line 3.
0638: A/c at N end of line 4.
0933: End of line 4. Recover magnetometer.
1058-1146: Conduct double figure of eight while awaiting TOBI preparation.
1146: S/c for start of first TOBI survey line (T).
1335: Launch TOBI and towed (buoyant) magnetometer at 28° 49.6'N, 43° 38.1'W, start of survey line T. TOBI running with starboard phase bathymetry only.
1600: XBT no. 11.

Friday March 15 (075)
0100: Discovered phase signal is useless because of signal overload and clipping; on-board gain controls not responding. Commence recovery.
0400: TOBI and magnetometer on board.
0415: S/c for SHRIMP site (28° 55'.9N, 43° 15'.9W), repeat of station S1.
0450-0716: Wire test of SHRIMP pressure cases. Wire test successful, but while rigging for subsequent station, discovered camera winds on uncontrolably, so station abandoned.
0920-0940: STCM figure of eight.
1115-1517: Dredge station D4 at 28° 57.2'N, 43° 12.5'W, ca. 2 km E of axis near S end of segment in zone of high magnetisation. Recovered slightly to moderately altered, glassy pillow lavas.
1612: XBT 12.
1627-1947: Dredge sation D5 at 29° 05.0'N, 43° 10.4'W, ca. 3 km E of axis nearer segment centre in zone of lower magnetisation. Recovered slightly to moderately altered, glassy pillow lavas.
2027: Deploy magnetometer and start overnight Simrad survey of eastern flank.
2057: WP S1.
2203: A/c, WP S2.
2318: A/c, WP S3.
2352: A/c, WP S4.

Saturday March 16 (076)
0121: A/c 184°, WP S5.
0355: A/c 309°, WP S6.
0502: A/c 024°, WP S7.
0630: WP S8; a/c 270° toward second TOBI line.
0949: Deploy TOBI and buoyant magnetometer. TOBI has modified wiring loom to try to suppress ringing in swath circuits.
1118: Starboard array failed: commence recovery.
1231: Magnetometer and TOBI inboard. Replacing modified loom by original.

1444: TOBI and magnetometer redeployed at 29° 03.68'N, 43° 33.80'W; start of TOBI line G.
1626: XBT 13.
1800: Discovered 'wire-out' value logged by TOBI is very inaccurate. Commence logging it by hand every 10 minutes. Sidescan, profiler and magnetometer running well; swath bathymetry from starboard side only, of variable quality.

Sunday March 17 (077)
1343: End of line G. Magnetometer recovered for turn. A/c clockwise to 270°.
1539: Start of TOBI line I. Magnetometer redeployed.
1627: XBT 14.

Monday March 18 (078)
1600: XBT 15.
1710: TOBI at end of line I: commence recovery.
1944: Magnetometer and TOBI inboard. TOBI team to work on swath bathymetry system. S/c 064° for SHRIMP/PINGER station over large fault scarp identified on CD65 TOBI.
2044: A/c to run along CD65 TOBI line.
2156: Launch SHRIMP with pinger on frame but no camera (u/s). PINGER station P1.

Tuesday March 19 (079)
0323: SHRIMP inboard; s/c for parallel line.
0355-0816: SHRIMP/PINGER station P2.
0816: S/c for start of TOBI line O.
1034: TOBI in water: Start of TOBI line O. S/c 090°, 2.0 knots.
1523: XBT 16.

Wednesday March 20 (080)
0800: End of line O. Commence recovery of magnetometer and TOBI for connection of port swath bathymetry. Moderate swell, wind 15-20 knots.
1145: Recovery complete, with minor damage to vehicle. Wind freshening to ca. 25 knots.
1258: TOBI and magnetometer redeployed.
1543: Passing waypoint at start of TOBI line M. Wind 30 knots.
1554: XBT 17.

Thursday March 21 (081)
Wind ca. 25 -30 knots, moderate swell.
1400: End of TOBI line M; A/c 090°; some initial difficulty attainining new trackline owing to strong northerly wind.
1544: XBT 18.
1724: Start of TOBI line Q; s/c 090°.

Friday March 22 (082)
1420: End of line Q: recover magnetometer, begin turn.
1530: XBT 19.
1547: Start of line S; deploy magnetometer, s/c 270°.

Saturday March 23 (083)
0000: Current surge and TOBI stops working. Begin recovery.
0254: Depressor weight on deck. Checks reveal short in slip ring assembly and open circuit at depressor end of umbilical.
0530: Repairs complete; redeploy TOBI; return to break-off point.
1138: Resume line S; s/c 270°; deploy magnetometer.
1542: XBT 20.

Sunday March 24 (084)
0559: End of line S. A/c 012° for line K.
0636: S/c 012°.
1007: A/c 090°.
1052: Start of line K. S/c 090°.
1540: XBT 21.

Monday March 25 (085)
0509: End of line K; recover magnetometer; a/c to port in poor weather.
1038: Deploy magnetometer; start of line E; s/c 270°.
1532: XBT 22.

Tuesday March 26 (086)
0924: End of line E; a/c to stbd.
1116: Start of line C; s/c 090°.
1130: TOBI logging computer stopped. Slow ship during repairs.
1456: Logging restarted; resume 2 knots.
1540: XBT 23.
1838: Weather worsening; recover magnetometer because fouling tow cable.
1916: Weather worsening. Captain considers change of course, but TOBI approaching passage between moorings D and B; commence hauling cable in case turn needed.
2015: Danger past; continue on 090°, veering cable again.

Wednesday March 27 (087)
0550: End of line C. Commence a/c to port in 30 knot wind.
0755: Start of line A. S/c 270°.
1530: XBT 24.
1857: Surface towed magnetometer stopped working: recovered and found unservicable.

Thursday March 28 (088)
0850: Simrad EM12 stopped logging.
0941: EM12 restarted.
1145: End of line A. Shorten TOBI cable in preparation for magnetic calibration turn..
1300: Deploy replacement magnetometer.
1312: Commence 450° turn at 5° per minute and 3 knots with TOBI at depth 250-350 m.
1452: Complete turn; s/c for start of line F.
1647: XBT 25.
1812: Start of TOBI line F; s/c 090°.

Friday, March 29 (089)
0800: End of line F. A/c to stbd.
1137: Start of TOBI line J; s/c 270°.
1534: XBT 26.
1734: Commence TOBI recovery for planned maintenance.
2042: TOBI on board after good recovery in 15 knot wind but heavy northerly swell; procede to dredge site.
2239: Commence Dredge D6, attempting to sample in-situ outcrop from deep on footwall of inside corner high.

Saturday March 30 (090)
0310: D6 completed; complete dredge lost (both weak links sheared) following ~ 5 ton 'bite'.
0356: Commence Dredge D7 at same site as D6.
0730: Dredge recovered: good haul including few pieces of gabbro (one with slickensides), possible indurated fault gouge, considerable quantity of altered basaltic talus, small amounts of dolerite, some indurated sediment, and few small chips of fresh basaltic glass.
S/c for resumption of line J.
0900: Commence TOBI deployment.
0930: Hydraulic power pack to starboard crane fails; jury-rig alternative.
1112: Resume deployment.
1155: TOBI deployed: resume line J.
1534: XBT 27.

Sunday March 31 (091)
0030: End of line J; a/c to starboard.
0151: Start of TOBI line H; s/c 090°.
1540: XBT 28: aborted.
1545: XBT 29: aborted.
2043: End of line H; a/c to starboard.

2358: Start of TOBI line L; s/c 270°.

Monday April 1 (092)
0000: Fault in TOBI; recover depressor weight; loop back to start of line.
0442: Depressor repaired (slip-rings shorted); resume line L.
1531: XBT 30.
2030: Another TOBI fault: recover depressor weight; continue on course 270° during repairs (slip rings again).

Tuesday April 2 (093)
0130: Depressor redeployed after repair. Deploy magnetometer. Pay out TOBI cable to 500 m.
0200: Conduct pitch calibration of TOBI magnetometer, veering and hauling.
0255: Calibration complete. Resume veering TOBI cable. Commence a/c to port for line N.
0400: Start TOBI line N; S/c 090°.
1545: XBT 31.
2146: End of line N; a/c to starnoard.

Wednesday April 3 (094)
0042: Start of line P; S/c 270°.
0520: TOBI failed: begin recovery.
0726: Depressor on board: repair slip rings. Maintain course.
1110: Depressor deployed; resume line P.
1410: End of line P; commence a/c to port to line U (270° turn).
1542: XBT 31.
1820: Start of line U, south to north along second major fault on W of median valley. S/c 023°.
2120: Waypoint U2; a/c 010°.

Thursday April 4 (095)
0205: Waypoint U3; a/c 017°.
0356: End of line U. A/c 090°.
0815: Start of line V, north to south along east flank of median valley.
0940: Waypoint V2; a/c 185°.
1352: Waypoint V3; a/c 180°.
1432: End of line V; a/c 222° to join line R.
1537: XBT 33.
1543: XBT 34.
1940: Start of line R (west): s/c 270°.

Friday April 5 (096)
0140: Commence last TOBI recovery.
0309: PES fish recovered.
0334: Magnetometer recovered.
0415: TOBI on board. Scientific watches ceased.
0430: All gear secured. S/c 059°, full speed to Ponta Delgada.
0904: Magnetometer deployed for passage.

Easter Sunday April 7 (098)
2340: Simrad EM12 stopped logging and switched off.

Monday April 8 (099)
0000: Magnetometer recovered: end of science observations.

TOBI Operations

(Ian Rouse and Chris Flewellen)

Instrumentation

TOBI - Towed Ocean Bottom Instrument - is Southampton Oceanography Centre, Ocean Technology Division's deep towed instrumented sidescan sonar vehicle. For this cruise the main scientific instruments on the vehicle comprised:

1. 30kHz sidescan sonar with swath capability (Built by IOSDL)
2. 7.5kHz profiler sonar (Built by IOSDL)
3. Three axis fluxgate magnetometer. (Ultra Electronics Magnetics Division MB5L)
4. CTD (Falmouth Scientific Instruments Micro-CTD)
5. Gyrocompass (S.G.Brown SGB 1000U)
6. Pitch & Roll sensor (G + G Technics ag SSY0091)

This was to be the first scientific use of the new swath bathymetry system. The system uses the signal transmitted by the existing sidescan sonar arrays but receives through dedicated swath bathymetry arrays, two on each side of the vehicle. Each 3m long swath bathymetry array consists of three rows of hydrophones, each row separated approximately half a wavelength from its neighbour in the vertical plane. The two arrays themselves are separated by approximately 8 wavelengths in the vertical plane.

Each hydrophone row is seperately amplified, TVG applied, filtered and passed to an Inpulse computer system where A/D conversion and quadrature sampling takes place. The phase difference between rows is measured and sent from the vehicle up the conducting cable to the ship via an FM link. The data is logged along with the normal sidescan and instrument data.

Also being used scientifically for the first time are the CTD, fluxgate magnetometer and gyrocompass. Although TOBI has always possesed a fluxgate magnetometer it was a prototype unit and not field supportable. This new unit is a commercial design and along with the CTD are standard items on both the SOC and RVS TOBI vehicles.

Prior to this cruise there was a trials cruise during which the new instruments were supposed to have been tested and calibrated. Unfortunately due to bad weather it was not possible to fully test the swath bathymetry or to swing the compass/magnetometer. These operations were planned for the passage leg to the work site but again bad weather stopped any deployments of TOBI.

During the trials cruise a problem of low signal to noise ratio was found in the swath receiving electronics. This was addressed during the port call in Lisbon and a main cause was found to be the use of a noisy filter circuit at the front end of the receiver. The ciruits were removed. Also achieved during the passage were the interfacing of the gyrocompass into the vehicle telemetry system and initial calibration and redesigned the profiler power amplifier drive circuitry to reduce the risk of MOSFET failure during the power down cycle.

Deployments

From day 68 to day 96 TOBI was fully deployed on 8 occasions. These are listed below.

Run	Start (GMT/day)	End (GMT/day)	Comments/Reason for recovery
1	10:45/68	13:20/68	Short circuit in electrical termination of main cable
2	14:25/69	08:45/70	Swath bathymetry test deployment
3	17:30/72	02:30/73	As 2 but initial deck problem with umbilical termination
4	13:45/74	03:10/75	As 2.
5	10:10/76	20:00/78	Single side swath.
6	10:50/79	11:02/80	Single line with one swath side.
7	13:15/80	19:00/89	Two sided swath run.
8	11:40/90	04:30/96	As 8.

The following is a more detailed description of each deployment, what we hoped to achieve and problems encountered.

Run 1

This was the first deployment and incorporated the modified swath pre-amps. We hoped that the removal of the noisy filters would give us a suitable s/n ratio to enable phase measurements to be made. The run was cut short after a high current condition occured at a depth of 350m. After recovering the depressor weight the problem was tracked to the electrical termination on the end of the main conducting cable. This was repaired with the vehicle still streamed behind the ship. After repair the system was turned on again but with no modem or instrument data telemetry occured. The vehicle was brought in and had to replace the zener protection diodes on the power supply card in the hydro tube. This is a common failure when a short circuit occurs. After re-installing the tube and testing on deck for 5 minutes another short circuit occured. This time it was in the deck lead being used. The umbilical was also tested and found to have an open circuit resistance of only 200kOhms. This should be many mega Ohms. The umbilical was changed, the hydro tube extracted again and the diodes replaced. On turning on the vehicle again there was still no modem or instrument data telemetry. The solution was finally tracked down to the top end power supply decoupling choke. This had burnt out and was replaced. All worked now after replacing in vehicle. Launched vehicle again but again a high current condition occured when power was applied. Recovered vehicle and took tubes out. After a lot of tests we came to the conclusion that the problem was due to the sea cable plug not mating firmly enough into the bulkhead connector on the hydro tube. This was exacerbated by the lack of a locking sleeve. The connector was changed and a locking sleeve added. Before the vehicle could be launched again the sidescan tube had to be opened and a profiler power amplifier MOSFET replaced.

Run 2

Deployed and everything worked at surface. During the decent to the seabed the Y magnetic signal failed and the pitch and roll sensors gave the same readings. The vehicle was run overnight with testing being conducted on the swath system. Poor s/n ratio was still evident on the swath signals which precluded any meaniful results being taken. Concluded that the filters were necessary to reduce out of band noise and prevent saturation of the signal. After recovery put back filters into pre-amps but at a later stage where their poor noise performance is not so damaging. The magnetic and pitch and roll problems were traced to trapped wires shorting together.

Run 3

Before the full launch a problem occured with noise and overcurrent on the main cable. This was traced to a bad electrical termination on the umbilical. Also had to replace the profiler MOSFET. During the run poor s/n ratio was still observed on the swath hydrophone signals.

Run 4

After run 3 ocsillation was observed on the outputs of the swath pre-amps. Decoupling resistors were added to the outputs. It was also found that plugging in both pre-amps together generated oscillation whereas plugging them in singley didn't. Decided to make this run with just the starboard swath array connected, blanking off the port side. The swath signal was now much improved. Not quite as good as the main sidescan signal but good enough for limited swath measurements to be attempted. On recovery problems were found with the Inpulse on-board computer system. Programmes were corrupted (bad hard disk) and a plug had come loose on one of the boards. These were corrected before the next deployment.

Run 5

One theory of the cause of the swath pre-amp oscillation was that it was due to the 'Y' connector harness wiring. The harness is designed to be reversable but this also puts signals from one pre-amp tube into the other pre-amp tube. This is not very hygenic and a custom harness was made from the spare. This was fitted for this run but a short on it necessitated a quick recovery and the original put on for the continuation of the run. Oscillation was observed on the sidescan signal during the run. On recovery pitting was visible on the sidescan tube with some pits 1.5mm deep. More work was done on the swath software and also a problem with phase stepping sorted out. The oscillation was probably due to condensation so thorough gassing with nitrogen and silica gel packs were used for the remainder of the cruise. The hydro tube showed signs of a low pressure dribble which were probably caused by a lack of 'O' ring crush on the end caps. The end cap clamps were resited to give more crush.

Run 6
Used the new design of 'Y' connector harness but due to an oversight the port pre-amp was not plugged in so it remained a single sided swath system. At the end of one line the vehicle was recovered to plug it in. During recovery in poor conditions TOBI was hit by the ship after going under the stern. The damage was luckily limited to a splinter off one of the buoyancy blocks and three bent buoyancy mounting rods. After inspection no immediate action was deemed necessary so redeployment went ahead. To prevent this happening again the ship kept forward speed throughout the final recovery phase.

Run 7
This was the longest run of the cruise and was only broken by a short circuit in the swivel on day 83. This was repaired without recovering the vehicle. During the run sidescan oscillation was observed when the vehicle was shallower than approximately 1500m. This wasn't too much of an inconvenience as most of the time the vehicle was deeper than this. The swath relative phase signal was reasonably good on the starboard side out to about half range and when there was a strong reflector on the port side as well.

Run 8
This run was punctuated by three swivel breakdowns. After the first the slip ring brush assembly was cleaned where the short had burned across, new oil put in and redeployed. The second occured 24 hours later. This time the brush assembly was changed and fresh oil used. The final breakdown occured 30 hours later. This time it was found that the bellows in the swivel body were only held in by loose screws. A new bellows unit was fitted and along with clean oil did the final 12 hours. All the above problems could be put down to ingress of water past the bellows unit. This having been fixed should be reliable again.

Commentary

The corrosion noticed on run 5 was stemmed by liberally coatinging the electronics tubes in vaseline. Despite this the corrosion got worse and areas 2mm deep were visible on the sidescan tube after run 8. The cause for this corrosion was probably a voltage leak to the sea water. although the actual cause of the problem was not found during the cruise.

Data from all the runs was recorded onto 1.2Gbyte magneto-optical disks. With the new data structure required to accommodate the swath data this gives a recording time of about 17 hours for each disk side. Throughout the cruise the old TOBI sidescan and profiler replay programmes were converted to run with the new data structure. A mosaic was made from the sidescan replays. Once a side of data was recorded it was transfered onto CD-ROM to enable it to be put onto the Sun processing system. This scheme worked well as not only was it easy to transfer the data but the CDs provided an instant archive record.

One annoying problem was with the TOBI wire out counter. This was interfaced to the ship's winch quadrature output. However when the winch was stationary the TOBI counter kept counting. This is probably a noise problem but no further investigations were undertaken as a manual 10 minute reading was adequate for processing purposes.

Another problem concerned the CTD/Gyro interface. Data from these serial instruments is gathered by an on-board microcontroller, converted and passed to the main vehicle data telemetry link. However below 1000m the pressure reading is corrupted occasionally. This only occured when the gyro data was being accessed as well. The problem lies in the microcontroller code but as the survey depth was always much greater than 1000m the problem did not manifest itself in the data set.

The gyrocompass was found to have an offset of 10.1 degrees referenced to the vehicle axis. This was assertained by comparing the recorded heading with the heading predicted by the TOBI track. The offset originates from the mechanical orientation of the instrument within its pressure sphere.

The lessons learned from this cruise are to improve TOBI's short circuit protection so that the protection diodes and the profiler MOSFETs do not blow. A gating circuit should cure the profiler problem and a dump circuit should prevent the diodes from blowing.

During the cruise TOBI was deployed for a total of 479 hours and collected over 14 Gbytes of data.

TOBI navigation

(Javier Escartin)

The location of TOBI along the tracks has been calculated using a simple trigonometric approximation. All the calculations are done in a ©Matlab program (navega.m). The input files for the program are the wire out, the ship position, and the depth of TOBI. navega.m calculates the position of TOBI and outputs files for plotting track charts, WHIPS processing, and re-scaling of the side-scan sonar for re-runs at ~ 1:50.000.

TOBI track calculation

TOBI navigation is calculated with navega.m, with the input from tobi_wirelog.dat, ship_nav.dat, and tobi_nav.dat. This program is based on positioner5.m, by Stefan Hussenoeder (WHOI).

The wire is assumed to be straight, and the lag of TOBI behind the ship can be calculated:

$$lag = \sqrt{(wire^2 - depth^2)} + 200$$

The length of the umbilical connecting the depressor weight and TOBI is 200 m. For the purposes of this calculation, the umbilical is assumed to be horizontal and at the same direction as the wire.

The angle of the wire is calculated at each time interval t = n. The angle depends on the previous position of TOBI at t = n-1, the ship location at t = n-1, n, and n+1, and a "viscosity" factor. The "viscosity factor" results in a smooth TOBI track (Figure 4, top). The latitude and longitude of TOBI are calculated from the location of the ship, the lag and the angle of the wire:

$X1_s, Y1_s$ Position of ship at time t = 0
$X2_t, Y2_t$ Position of TOBI at time t = 0

$X3_s, Y3_s$ Position of ship at time t = -1
$X4_s, Y4_s$ Position of ship at time t = 1

From which α_{12}, α_{23}, α_{31}, α_{14} and are calculated:

$\alpha_{12} = atan(Y1_s - Y2_t, X1_s - X2_t)$ Angle between TOBI at t = 0 and ship at t = 0
$\alpha_{23} = atan(Y2_t - Y3_s, X2_t - X3_s)$ Angle between TOBI at t = 0 and ship at t = -1
$\alpha_{31} = atan(Y3_s - Y1_s, X3_s - X1_s)$ Angle between ship at t = 1 and ship at t = 0
$\alpha_{14} = atan(Y1_s - Y4_s, X1_s - X4_s)$ Angle between ship at t = -1 and ship at t = 0

The new angle α_n is:

$$\alpha_n = \{((mul + vis\ \alpha_\phi)\ \alpha_{12}) + \alpha_{23}\} / \{mul + vis\ \alpha_\phi + 1\}$$

where $\alpha_\phi = (\alpha_{31} - 2\pi) - \alpha_{14}$, and *mul* = 0.3 and *vis* = 300. These variables produce TOBI tracks that are smooth. Lower values of *mul* result in TOBI tracks that follow more closely the ship track (less smoothing).

Calibration of TOBI heading and accuracy of navigation

TOBI heading from the gyro and the heading calculated from the TOBI track are compared in the middle of Figure 4. The calibration factor for TOBI gyro for the whole profile is -10.15° (Figure 4, bottom). The lack of any systematic difference in the heading offset between the eastward and westward tracks indicate that TOBI follows the ship track closely, and that it is not being displaced laterally substantially by currents. In addition, there is good agreement on the pattern of heading changes (Figure 4, middle) suggesting that the calculated TOBI positions are accurately predicting the flight of TOBI.

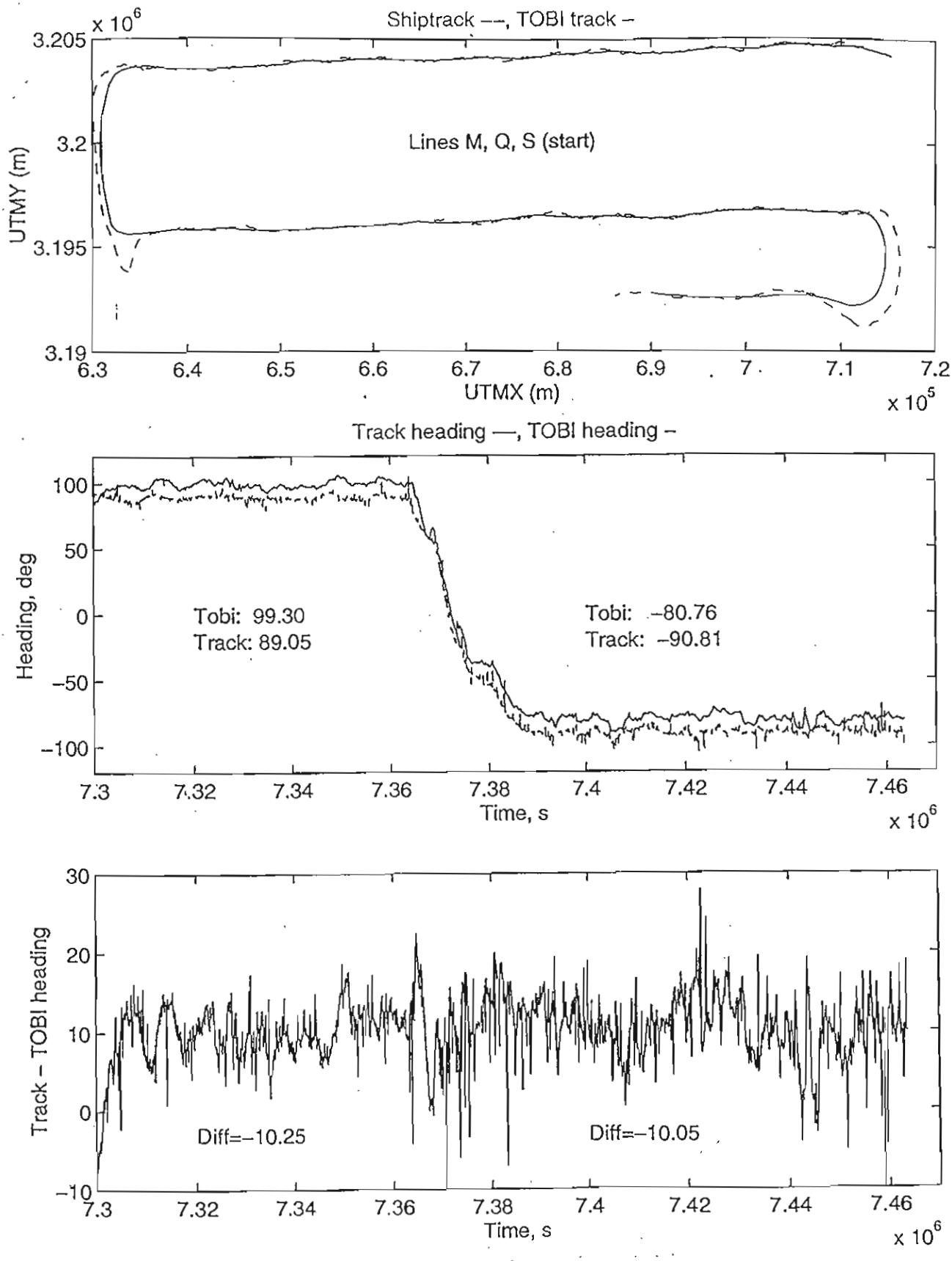

Figure 4: TOBI navigation. Top: ship's track (dashed) and TOBI track (solid) computed as described in text. Middle: Comparison of TOBI heading deduced from the calculated TOBI track (dashed) and taken from the TOBI gyro (solid) through a 180° turn. Bottom: Difference between the TOBI heading deduced from the calculated TOBI track and that taken from the TOBI gyro, over the same time period as displayed in the middle panel.

Input files

Wire out data

Wire out is logged by hand every 10 minute. The data is input into a text file (e.g., tobiKE_wirelog.dat) that contains four columns with the Julian day, hour, minute, and wire out in meters. The text must contain no text characters in order to be readable by Matlab:

tobiKE_wirelog.dat:

```
77  05 15     2345
77  05 18     2500
77  05 20     2500
77  05 24     2500
77  05 30     3630
```

Ship's latitude, longitude

Ship location is extracted from the files maintained on-board, using the listit command:

```
listit -s 960770515 -e 960781012 -k good bestnav lat lon >! ship_nav1.dat
awk navega_ship.awk ship1_nav.dat >! ship_nav.dat
```

listit creates a file with location every second or so. The start time (-s 960770515) must be smaller than the start time of the wirelog. The end time (-e 960781012) must be larger than the end time on the wirelog. This is required to interpolate the location of the ship over the time period determined from the wirelog. The listit start and end times must be modified accordingly in navega_extract.m

The awk command decimates the file and produces an ASCII file readable by Matlab. The formatting statement is in navega_ship.awk.

TOBI depth

TOBI depth is extracted from the ASCII files created for each of the raw files (/data22/CD99/cd99p*.mag). navega_extract.m decimates each of the raw files decimated with awk (formatting statement in navega_tobi.awk). The decimated files are combined into a single file tobi_nav.dat. navega_extract.m has to be modified to incorporate the different cd99p*.mag files.

```
awk -f navega_tobi.awk /data22/CD99/cd99p22.mag >! tobi_nava.dat
awk -f navega_tobi.awk /data22/CD99/cd99p23.mag >! tobi_navb.dat
awk -f navega_tobi.awk /data22/CD99/cd99p24.mag >! tobi_navc.dat
cat tobi_nava.dat tobi_navb.dat tobi_navc.dat > tobi_nav.dat
```

The start time of tobi_nav.dat must be smaller than the start time of the wirelog. The end time of tobi_nav.dat must be larger than the end time on the wirelog. This is required to interpolate the depth of TOBI over the time period determined from the wirelog

Output files

file_list

The variable file_list corresponds to the name of the file used for the plotting of tracks at 1:50000 on the pen plotter. These tracks are used to construct the TOBI side-scan sonar mosaics. The output contains year, Julian day, hour:minute:second, TOBI latitude (format 11e) and TOBI longitude (format 13e):

```
96 078 12:14:20 2.90000e+01 50 -4.30000e+01 50
```

The values of 50 after the lat and lon are required for RVS plotting programs.

file_whip

This file is for the whips processing program. It contains cruise name, year, month, day, hour, minute, second, TOBI latitude, TOBI longitude, wire out, ship's heading (degrees), and ship's speed (m/s) over the ground (the last two variables are calculated from the ship's navigation files):

CD99-1996 960315 1214 29.000 -43.000 3500.00 45.00 1.89

file_scan

This file is needed by TOBI team to re-play the side-scan sonar data at 1:50.000, so that it matches the TOBI track plots to construct the mosaic. The output is year, Julian day, time interval, x position, y position, and total distance for the time interval. All positions and distances are in mm, corresponding to the actual distance at 1:50000.

TOBI Swath bathymetry: theory and results

(Chris Flewellen)

Theory

The back-scattered signal arriving at TOBI is highly coherent over a vertical scale much greater than the dimensions of the vehicle. It is possible to calculate the arrival direction of the returning echoes by measuring the time difference (or, equivalently, the phase difference) between signals received at two vertically separated hydrophone arrays. The accuracy of the measurement improves with increasing separation (it is about 8 wavelengths for TOBI - see below) although this results in an ambiguous phase difference. The scheme adopted for ambiguity avoidance on TOBI was to delay sampling the upper array relative to the lower. If an estimate of the expected time delay can be derived that aproximates to the actual time difference, the phase difference between the two signals can be kept within the range + π to - π. If this differential phase difference is then added to the phase function used to generate the time delay, the total phase function is recovered.

Each array contains three rows of elements spaced by aproximately half a wavelength (Figure 5). The phase difference between adjacent rows is thus less than 2π and therefore unambiguous. An unambiguous phase difference equivalent to a spacing of 2 wavelengths can be generated by adding the four row-to-row differences. This phase signal can then be scaled up by a factor of about four to provide the estimate of phase difference, and hence time delay, required over the total eight-wavelength aperture. Alternatively this signal could be transmitted up to the ship to provide a noisier but unambiguous signal from which the arrival angle could be calculated.

As the total phase difference spans about 3000° (8π), but needs to be resolved to about 1°, it is compressed for transmission up the cable. This is acheived by translating the signal into depth below TOBI, as a function of range. This process can be inverted on the ship to provide the phase angle again.

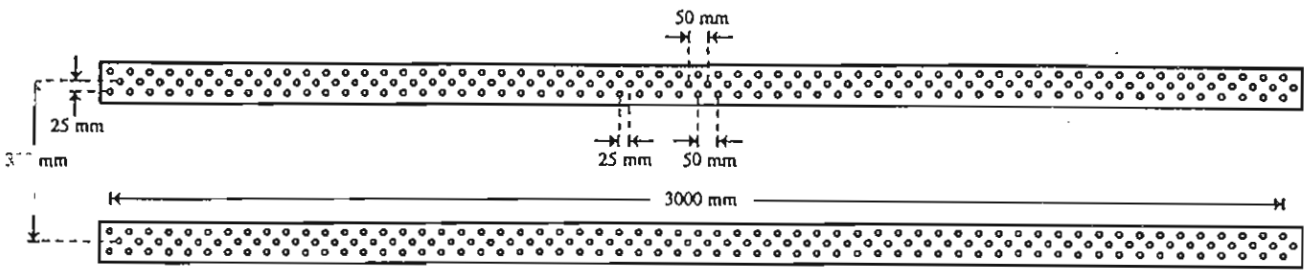

TOBI swath bathymetry sonar arrays
(side view)

Figure 5: Layout of the new TOBI bathymetry transducers.

Hardware

TOBI was thoroughly modernised for this cruise. In addition to the classical "side-scan" transducers, six new rows of "bathymetry" transducers were installed on each side. The side-scan units each consist of two rows of parallel-connected transducers with a vertical separation of 25 mm, inclined downward at 20° from the horizontal. These units were all connected together and they furnished the sonar output pulse used for sidescan and bathymetry, and received the side-scan signal.

The bathymetry transducers are used for reception. They are arranged in two groups of three rows of elements (arrays) on either side (Figure 5). Each row has 60 elements spaced 50 mm apart horizontally. These elements are connected in parallel for the whole row. The three rows in each group are 25 mm apart vertically (about $\lambda/2$, where λ is wavelength,), and the group centres are 398 mm apart vertically (approximately 8λ). The new arrays are mounted in a vertical plane, with the transducer axes ('bore-sights') horizontal.

The side-scan arrays transmit sonar signals at 30.37kHz (starboard) and 32.25 kHz (port). The vertical array spacing within each group of the bathymetry arrays is thus approximately $\lambda/2$. To obtain a horizontal array spacing of $\lambda/2$, the adjacent rows are staggered 25 mm and their outputs are weighted 1:2:1.

Results and problems

Despite two previous trials cruises (November 1995 and February 1996), it was not possible to get the system working properly during CD99, let alone calibrated. For most of the time some phase information was logged in the hope that subsequent processing could extract some depths, if only over a narrow swath.

On the first trials cruise we were not ready to launch TOBI until the last day. When the power was turned on, the new gyro hogged the current and prevented various power supplies from starting up correctly. The result : the side scan transmissions were disabled and the swath processor hard disc drive crash landed, ruining a crucial boot-up file. There was no way to communicate with the processor to repair the damage.

During the second trials cruise we had open circiuts and short circuits in two umbilicals and a rusting tow-cable. That tow-cable was eventually discarded. The profiler power amplifier (not a TEAM TOBI design) automatically blew up whenever there was a short circuit on the cable.

The swath hydrophone pre-amplifiers had to be rebuilt because of exceptionally noisy filter circuits. There was instability in the time-varied gain applied to the pre-amps and an oscillation which is still proving difficult to track down as it only happens when the vehicle is in the water. [Subsequently located on cruise CD100?]

During CD99 the replacement hard disc drive had many bad sectors and various programs would not run properly. A further replacement disc drive would not work without contentions with other hardware.

The electronically controlled potentiometers used to control the gains of the individual hydrophone rows were prone to ramping up and down by themselves and were enventually removed from the circuit. The analogue-to-digital converters, each sampling 12 channels port and starboard, were inclined to channel hop so that pairs of in-phase and quadrature samples were incorrectly identifed, resulting in garbage phase information. The starboard analogue-to-digital converter developed some open circuit connections that came and went as the board was manipulated. It took a steady hand, good eyesight and a very fine pointed soldering iron to make the repair.

In addition there were some human errors in the software and in the wiring up of some plugs and sockets.

Summary

A lot of problems have been solved though it would have been better to have solved them before a major science cruise.

TOBI swath bathymetry: processing

(Peter Slootweg)

Introduction

During CD99 two types of phase signals were produced. The "unambiguous" phase was obtained by summing the phase differences of the four adjacent bathymetry array pairs that are $\lambda/2$ apart (i.e., two pairs in each group). The "ambiguous phase" is obtained by measuring the phase difference between the two signals from each group, obtained by weighted addition of the signals from the three rows in the group. The phase signals were sampled at the same rate as the sidescan sonar signal (4000 samples per side per 4s sweep) and logged in the TOBI record.

The unambiguous phase signal has a one-to-one relationship with the angle of incidence of the backscattered wavefront. An angle of 0° (horizontal) corresponds to a phase difference of 0. For an angle of 90° (vertically down), the phase difference across each pair of rows is $\pi/2$, and since the phases from four pairs are added, the total phase difference is 4π. Unfortunately the unambiguous phase shows a high noise content and the large dynamic range causes a limited precision after reducing the signal to the standard 12 bit format coming up from the vehicle.

The ambiguous phase is so-called because the aperture used to measure it (398 mm) is larger than half a wavelength, so the phase wraps around when reaching π. There is no longer a one-to-one relationship between phase and the angle of incidence. However, the ambiguous phase has a better resolution than the unambiguous phase because of the larger aperture (398 mm versus 100 mm), which is less affected by the reduction to 12 bit because the dynamic range is limited to $-\pi$ to $+\pi$. In addition, it was possible to "reduce" the ambiguous phase by subtracting the phase variation expected for a level, horizontal seafloor, thus decreasing the dynamic range of the signal.

Before it can be used, the ambiguous phase has to be "unwrapped", i.e. phase changes of 2π must be removed by adding the correct multiple of 2π. If the signal is noisy, the result of unwrapping is of limited value. Another problem is posed by zones where the strength of the backscattered signal is low. There the noise in the phase increases. This is particularly true for shadow zones and in the water column, where no signal is scattered at all.

Raw swath bathymetry data formats

The format of raw TOBI data changed at the start of the cruise from the previous version (number 6) to the current version (8), necessitating a major change in various sidescan sonar processing programs. However the format did not change significantly during CD99 except for the *content* of the raw swath records.

The raw swath records would contain one of the following: [Peter - can we add the times for which each applied?]

1. 2×3850 samples of depth below the vehicle versus two-way travel time. These estimates of depth were generated in the tow-vehicle.
2. 2×3850 samples of ambiguous phase reduced to a constant altitude (200 or 400 m).
3. 2×3850 samples of ambiguous phase without reduction.
4. $2 \times$ (1875 samples of ambiguous phase + 1875 samples of unambiguous phase) with the original sampling rate (but over only half the usual swath width).
5. Same as 4 but undersampled to cover the original swath width.
6. Another combination used during the testing phase (not analysed).

Various errors and noise sources were identified with these different data types: full details are given in the table on page 61.

These different signals needed careful analysis to ascertain that they contained the correct values. During CD99 there were some uncertainties as to the sign convention being used. More importantly, the unambiguous phase has a phase jump of 4096 (representing somewhat over 2π) at a certain range on both sides, and the port unambiguous phase has additional, arbitrary jumps at various ranges.

After returning home we found that in type 6 the 2000 samples of ambiguous phase had been sampled at the sidescan interval but with the amplitude reduced to 50% of its original value.

The noisy nature of the signals make this kind of analysis difficult: typically 2000 pings of 2 × 4000 samples each (32 Mbyte of data) have to be analysed together to get enough statistics and avoid the influence of local bathymetry. This can only be done graphically.

Meanwhile, we have manually corrected the phase wraps on a sample of the ambiguous phase data to produce a first bathymetric map (see frontispiece).

The data used are ambiguous phase recorded to half range, starboard side, from part of one of the E-W lines crossing the western median valley wall near the southern end of the segment.

1. First, the phase wraps (which separate 'fringes' where average phase changes by 2π) are identified by eye and digitised on the image of raw ambiguous phase data. An arbitrary value of $2n\pi$ is given to the first fringe, increasing by 2π at each wrap.
2. The matrix of identified wraps is added to the ambiguous phase to obtain a continuous phase matrix. $\pm 2\pi$ is added to those points more than $|2\pi|$ from the local median value to bring them within $\pm 2\pi$. The standard deviation is calculated for the whole section, and points that fall more than 2σ from the local median value are removed.
3. As there is ambiguity on the absolute zero phase, we compute the depth below TOBI for the 'unambiguous phases' assuming different starting $2n\pi$. If the chosen n is too low, negative ranges are obtained and can be discarded. Too high n yields unreasonably steep depth profiles.
4. Bathymetry is calculated by adding the depth of TOBI to the depth below TOBI computed from the phases.

Bathymetry processing modules

To cope with the new bathymetry data, some changes were made to the WHIPS (Woods Hole Image Processing System) processing package that had been in use by SOC for processing TOBI data.

Raw2whips modules

The *raw2whips_bathy2* module was written to collect phase data from the raw files and convert them into a WHIPS netcdf "image" for viewing (by *viewwhips*) and further processing. This *raw2whips_bathy2* program only copies the input without modification and builds a corresponding WHIPS header.

A second module *raw2whips_bat2* was written to accommodate the different contents mentioned above, and to do advanced processing (bottom detection, median filter, boxcar filter, phase unwrap, conversion of phase to depth), generating a WHIPS image of depth below TOBI versus time.

One of the options included is to use the unambiguous phase to predict the correction (unwrapping) for the ambiguous phase if both are given in the raw file.

Normally several of these operations would be done in separate stand-alone WHIPS programs, but because the side-scan is used in several different ways it was decided to combine the operations into one front-end. As in other WHIPS modules, the operations on the data are called for by command line options.

The 24 options of *raw2whips_bat2* make it awkward to operate. The bottom detection (operating on side-scan) needs improvement, and median filtering of ambiguous phase should be done (in 2 dimensions) on parallel traces. The module should also suppress output when the sidescan signal is low (shadow zone). The latter feature has been programmed but not yet tested.

Tobbat module

The slant-range correction is done in a separate WHIPS module, *tobbat*, modelled on *tobslr*. It performs slant-range correction by calculating the angle of incidence, correcting for vehicle roll, ray tracing to slant range using a simple velocity structure, and interpolation of the resultant points on to a WHIPS image after adding vehicle depth. This module was completed but not fully tested before the end of CD99.

Final remark.

One of the difficulties in using phase-related data in WHIPS is that WHIPS is not equipped to deal with images with data gaps in the middle (shadow-zones). It is actually possible within the netcdf structure to identify special values as "no_data" and use them as such in a regular way. Future releases of WHIPS should use the possibilities given by the netcdf structure more fully than is done now.

On-board TOBI sidescan processing

(Roger Searle and Peter Slootweg)

WHIPS processing of sidescan data

We had kindly been supplied a copy of the WHIPS processing package developed by Tim LeBas at IOSDL/SOC for TOBI sidescan processing. This contains a number of routines for performing various processes which can broadly be divided into those applied before mosaicking (e.g. slant-range correction, drop-out removal) and those applied during mosaicking (geographic projection and registration, etc.) In fact mosaicking involves two processes: WHIPS will project images into geographic maps, but will make separate maps if images overlap. Therefore another package must be used for overlaying one map on another and defining the way each is cut at the overlap. We planned to use ERDAS-Image for this, but did not reach that stage on board. These processes can all be run individually, but WHIPS also provides a number of rather complex shell scripts (e.g. process_tobis) which will automatically process a whole survey, and are designed to be used at the end of a cruise.

Because the TOBI recording format had changed to incorporate the phase bathymetry, it was necessary to make a number of changes to the WHIPS routines. Usually, where these were originally labelled *_tobi, the new equivalents were called *_tobi2. The opportunity was also taken to allow for future developments, e.g. incorporation of the pahse bathymetry into the slant-range correction procedure. These changes were carried out by Peter Slootweg at the beginning of CD99.

On this cruise for the first time TOBI data were downloaded onto writable cd-rom by the TOBI team. Each disc held up to 17 hours of data, usually in one but sometimes in multiple files.

During the course of the cruise we routinely converted the cd-rom files to net-cdf files for processing by WHIPS, and ran a number of the individual WHIPS processes to check on their operation. At the end of the survey we attempted to post-process all the sidescan with process_tobis, but ran into various snags which we were not able to entirely resolve in the time remaining.

Navigation

Ship navigation was taken from file 'bestnav' provided by the RVS computer system, and made available in a 'dxfmt' file in directory /dxf (linked to the RVS computers). One must convert this to ASCII using unix command 'fold' (fold dxfmt.* > cd99.nav) and move cd99.nav to the /nav directory.

TOBI navigation was provided by a WHOI program (see separate section of this report) and also placed in the dxf directory under names such as cd99xxx_tobi.nav, where xxx identifies the time span or TOBI file numbers. These files must be concatenated (in date order) and moved to directory /nav, where we named the concatenated file cd99.veh_jav. Finally, in directory /nav, remove earlier versions of cd99.veh_nav and cd99.cable (if they exist), and type 'wireout cable'. This will prompt for length of cable out, but any value can be input - it is not used. (wireout formally calculated the TOBI positions from wire out, but now is used just to format the files properly).

These navigation files can be created daily or at longer intervals as needed. They must exist before running process_tobis.

Noise removal: noisecut_tvg

One feature of the TOBI files on this cruise was a rather large amount of noise at far range, particularly on the starboard side. This was clearly being amplified by the time-varied gain applied. The level varied gradually throughout the cruise. Simple division of the signal amplitude could have removed it, but at the cost of unduly reducing the signal while maintaining the same signal-to-noise ratio. Instead, we *subtracted* a correction based on the tvg law. This will slightly reduce the signal level, but since no usable signal can be seen much below the level of the noise this is not a problem in practice.

A new WHIPS routine noisecut_tvg was written by Roger Searle to apply this correction. It was based on one of the existing 'shading' routines. The correction was calculated as follows:

The tvg gain, in decibels, is given by

$$g\ (\text{dBel}) = 40 \log_{10}(0.75t) + 0.005428\ t, \tag{1}$$

where t is the one-way travel time in milliseconds.
To obtain logged voltage, divide by 20 (not 10) and exponentiate:

$$g\ (\text{V}) = (0.75t)^2 \times 10^{0.00027264t}. \tag{2}$$

Our data were subsampled to 1000 samples per ping, ranging from $n = 1$ at far range starboard to $n = 1000$ at far range port, so

$$t = (501 - n) \times 8 \qquad [n \leq 500, \text{starboard}] \tag{3a}$$
$$t = (n - 500) \times 8 \qquad [n > 500, \text{port}]. \tag{3b}$$

If g_{max} is the value of g at maximum range, the *relative* gain (from 2 and 3) is:

$$g/g_{max} = ((501 - n)/500)^2 \times 10^{0.00027264(4008 - 8n)}$$
$$= (1.002 - n/500)^2 \times 10^{(1.09274112 - 0.00218112n)} \qquad [n \leq 500, \text{starboard}]. \tag{4}$$

In routine noisecut_tvg, this expression is evaluated to create a look-up table (and symmetrically for port side). Then, for each pixel, the quantity

$$noisecorrn = noisemax \times g/g_{max} \tag{5}$$

is subtracted from the logged value,

where *noisemax* is the observed level of noise at maximum range. The maximum noise value (noisemax) on port and starboard sides can be set independently, either by default in the program or as command-line arguments, and should be based on measured values. It may be necessary to run noisecut_tvg several times with different values of noisemax and view the results before deciding on a final value for *noisemax*. We used values ranging from 100 to 200 on the port side and 300 to 800 on starboard. Currently the defaults are 100 and 700. We applied noisecut_tvg to all files immediately after the alline stage (see below). For comparison, maximum loggable signal is 4096 (12 bits).

Suppresion of sea-surface reflection: suppress_tobi2

A WHIPS routine called suppress_tobi2 is available for removing the sea-surface reflection and replacing it by interpolated values. This was not originally available in process_tobi, but has been incorporated in a revised script called process_tobis. A problem with this routine is that it cannot work on a reflection within a specified distance (~100 m) from the nadir or edge of the image. As we received it, it would simply exit if it encountered this situation. We modified it to simply skip lines where this condition occurred, and found that, since there is a degree of along-track averaging, this was able to suppress almost all of the unwanted reflection. Specify -p to use the pressure reading to estimate position of the reflection.

Shading: shade3gen_tobi, shade3_tobi, etc.

'Shading' in TOBI jargon means applying a range-dependent gain correction to even out the combined effects of incorrect TVG, beam directivity, angular-dependent reflectivity, etc. There are various ways of doing it: we tried most of them, and came to the conclusion that they make matters worse! To avoid applying a shading correction, specify 'shade0' when prompted by process_tobis. However, we think you still need to have a 'cruisename.shade3' file in the appropriate directory!

Removing line dropouts: drpout

This routine removes line dropouts by interpolating across lincs of unusually low signal strength. The documentation implies that it can be run using only a threshold argument -t, but we found this won't work unless you specify -f as well. process_tobis as supplied uses drpout -u -f -k, but we found this did not work, and just specifying -f (allowing default threshold) worked best.

Viewing netcdf files: viewwhips

Usage: viewwhips netcdf_filename. viewwhips is based on Xview, and is for viewing TOBI files on screen. Click middle mouse button on image to get 'colour editor', and set gamma = 3 for optimal contrast. Left mouse button displays image coordinates.

Filenames

Raw files (from cd-rom) have sequential numbers given by the TOBI team (not starting at 1!). We labelled the raw files things like tobi.*n*.raw, and the converted files cd99p*n*.cdf0, where *n* is a sequential integer starting at 1. All subsequent filenames started cd99...

Other processing

Other useful routines include the following, in the order applied. Command line arguments are typically: -i input_file_name, -o output_file_name, -H (show help information and other arguments).

raw2whips_tobi2	Converts from TOBI format to netcdf. Do this before you can do anything! We put the cd-rom files in directory /raw (with extension .raw) and converted files in /cdf with extension .cdf0.
raw2mag_tobi2	Converts magnetic data from TOBI format to unix. Specify -r for 'raw' format.
alline:	Pads out files to ensure that each starts on an even minute and has scans 4 s apart with no gaps. This should be run before process_tobi, and is usefully run daily. We put the results of this in /alline, labelled *.cdf.
noisecut_tvg	See above. Results put in directory /nct and called *.cdf. Also run daily.
shade3gen_tobi	(If you must) Generates a shading file. Follow instructions in TOBI documentation, and choose a long, representative image as a 'training' area, not a short subset. We think (both on theoretical grounds and on the evidence of trying it both ways) that this should be run *after* slant-range correction.
dk2dk_tobi	Create a subset of an image. Useful for viewing small parts at a reasonable scale and resolution.

The following *may* be run 'manually', but are all included in process_tobi and will be done if you run that at the end of the cruise:

tobtvg2	Originally run to smooth the tvg, but now used for a variety of smoothing functions, depending on argument.
mrgnav_tobi2	Merges ship and/or TOBI navigation into the TOBI image files for use in subsequent processing.
tobslr	Apply slant-range correction. Must first run tobtvg2 -a to smooth the altitude data, mrgnav_tobi2 -n ship_navigation_file -s, and mrgnav_tobi2 -n TOBI_navigation_file -t -w (see above, 'navigation').
shade3_tobi	(If you must) Apply the shading correction. We think this should be applied *after* slant-range correction.
suppress_tobi2	Suppress sea-surface reflection (see above).
drpout	Removes line dropouts. Specify -f (see above).

Various other routines are used by process_tobis, but are not useful for everyday work.

TOBI magnetometer measurements

(Simon Allerton and Simon Russell)

Instrumentation

Three components of the magnetic field are measured on TOBI, using a system of three orthogonally-mounted fluxgate magnetometers. Orientation measurements are provided by a gyrocompass and two orthogonal tiltmeters, recording heading, pitch and roll. Magnetic and tiltmeter measurements are made every 0.5 s. Heading is recorded every 2.5 s.

The gyro and tilt meters are not precisely aligned with the TOBI, indicated by surveying compared to the ship system (true head = tobi head -8.8deg), and by comparing the mean ships heading and the TOBI heading on reciprocal bearings (true head = tobi head -10.25deg). See also the section on TOBI Navigation. This misalignment produces a correlation between the pitch and the roll. Further misalignment of the magnetometers may cause further correlation problems, which have not yet been fully investigated. Pitch measurements are recorded in the range $\pm 20°$, saturating outside this range.

TOBI's contribution to the magnetic field has been assessed by a series of calibration experiments which are described in more detail below.

Initial problems with data recording resulted in the loss of the first 4 bits from each magnetometer voltage signal. This effected the Test Line and Line T (12.03.96 - 15.03.96, files cd99p2-3). It should be possible to restore these data by by adding a multiple of 2^{16} to the data to correspond to the IGRF. First attempts to rectify this problem in the towfish caused a loss of the last 4 bits of data (16.03.96 - 18.03.96), causing a loss of essential resolution. These data cannot be used (Lines G and I, files cd99p4-8). Data recorded from 19.03.96 onwards are generally of high quality, with a low signal-to-noise ratio. Apart from removal of rare data spikes, no filtering was necessary.

Calibration of three component fluxgate magnetometer

Theory

In deep-tow work the sensors are far enough away from the ship for it to negligible effect, but the tow-vehicle itself produces its own magnetic fields. Although TOBI is made of essentially non-magnetic materials, there are some components that are magnetic, for example the gyro, and therefore have a magnetic moment. The three fluxgate sensors therefore measure not only the geomagnetic field but also the magnetic fields produced by the induced and permanent magnetic moments of any magnetic materials within the region surrounding the sensors.

The observed vector field, $\mathbf{H}_{ob}$, can be thought of as the sum of geomagnetic field, $\mathbf{F}$, the magnetic field produced by the induced magnetic moment of the vehicle, $\mathbf{H}_i$, and the magnetic field produced by the permanent magnetic moment of the vehicle, $\mathbf{H}_p$:

$$\mathbf{H}_{ob} = \mathbf{F} + \mathbf{H}_i + \mathbf{H}_p$$

The Earth's field $\mathbf{F}$ is a weak field, therefore $\mathbf{H}_i$ is proportional to $\mathbf{F}$. This only holds outside the magnetic body itself which is the case for the fluxgate sensors. For durations as short as the time of the suvey the field produced by the permanent magnetic moment, $\mathbf{H}_p$, can be asumed constant. The field produced by the induced magnetic moment is not constant and is a function of vehicle attitude as well as the external applied field.

The method used to remove the vehicle's magnetic effect from the obsevations is an empirical method based on the above equation. Theoretical methods, such as the method of Isezaki (1986) to correct the shipboard three component magnetometer for the effects of the ship's magnetization, can also be used for deep tow magnetics.

Calibration experiment

In order to remove the magnetic effects of the vehicle, it is necessary to record the magnetic field in a region where there are no anomalies and when the vehicle has the most varied attitude. The location of the experiment was determined from the surface magnetic chart in a region where anomalies and horizontal gradients were a minimum. The region around 29.17°N, 43.62°W was the

best region within plausible limits, although ideally the calibration should be done away from the ridge axis in a magnetic quiet zone, e.g. the Cretaceous magnetic quiet period.

Variations in vehicle attitude can be resolved into the three orthogonal motions of yaw, pitch and roll, which can be treated independantly. To obtain variations in heading the vehicle was towed in a loop through at least 360°, at a depth which was far enough away for the magnetic effects of both the ship and any subsurface magnetic sources to be ignored. For water depths of a few kilometers it is sufficient to have between 500 m and 1000m of wire out. This puts the vehicle at a depth of approximately 200 m to 300 m when the ship speed is 2 knots and turning at 5° per minute. To obtain variations in pitch it is necessary to haul in and pay out the wire whilst turning on the loop. A wire rate of 30 m/min was sufficient to cause variations of ± 7° in pitch, which covers most but not all of range observed during the survey. We also carried out a second experiment to assess the effects of variation of vehicle pitch. This was carried out in a straigh line at 28.97°N (at the western end of line L) between 43°31.95'W and 43°32.67'W, with in excess of 500 m of wire out. The ship speed was 1 knot. The vehicle was made to pitch by hauling in and paying out at 40m/min. Together these two experiments enabled us to obtain pitch variations of ± 20° over heading variations of approximately 270°.

Variations in roll were ignored since the vehicle's roll rarely exceeded ± 0.5°, which can be considered negligible.

Processing scheme

1. Calculation of total field from the three fluxgate readings.

2. Removal of 10.25° from heading (see above).

3. Correction for the *geometric* effects of pitch. Let the old coordinate system be fixed to TOBI with x toward the nose and parallel to TOBI's fore-aft axis, y to starboard and z down. This system rotates with TOBI. The new coordinate system is independent of pitch and consists of X horizontal in the fore-and-aft vertical plane of TOBI, Y horizontal towards starboard and Z vertically down. This system does not rotate with pitching movements of TOBI, but the directions of X and Y are functions of the TOBI heading. We make the assumption that roll of TOBI is negligable so no correction is made to the y component. The conversions for x and z are:
X = x.cos(p) - z.sin(p)
Z = x.sin(p) + z.cos(p),
where p = pitch.

4. Calculation of IGRF values for the location of the loop (29.17°N,43.62deg). This was done using a routine that extrapolates the 1990 values for a given Julian day, year and position. The calculated values for north, east, vertically down and total field IGRF are:
IGRFN = 26121.3 nT
IGRFE = -8064.9 nT
IGRFD = 30848.3 nT
IGRFT = 41218.7 nT

5. IGRF was then calculated for the given directions of the X, Y and Z readings every 2.5 seconds:
IGRFX = IGRFE.sin(h) + IGRFN.cos(h)
IGRFY = IGRFE.cos(h) - IGRFN.sin(h)
IGRFZ = IGRFD,
where h = heading.

6. The difference between the calculated IGRF vector and the observed magnetic field vector is the magnetic field due to the vehicle. This is not constant but is a function of heading and pitch due to the component of induced magnetisation ($\mathbf{H}_i$ above).

7. For each component and the total field a truncated Fourier series was fitted to the data (Figures 6 - 9). The number of terms in the Fourier model should be 3 (a constant, sine of the heading and cosine of the heading) for each of the components and 5 (a constant, sine and cosine of the heading and sine

and cosine of twice the heading) for the total field (Bullard and Mason, 1961). Because the loop consisted of a more than 360° turn, parts of the curve are duplicated, with some heading values associated with both small pitch values and large pitch values. At these places the effects of vehicle pitch in the signal become very obvious. Because the pitch data are scattered around zero, the Fourier models describe the heading correction for instances when the vehicle is not pitching. These are then subtracted from the profile data as the heading correction.

8. The difference between the theoretical Fourier models and the obsevations was calculated for each of the components and the total field. The difference, or residual, is the magnetic effect of the vehicle, which varies with pitch. For small pitch angles the relation between anomaly and pitch should be linear. However, the data plot was very scattered, especially for the individual components (Figures 10, 11). A more detailed investigation is needed. Nevertheless, a linear trend for the total field data was determined and estimated to be:

$$\text{Pitch anomaly (nT)} = -19.43 \times \text{pitch}(^\circ) + 10.0.$$

This pitch correction was then applied to the data

Magnetic Data Processing

The processing routine for the magnetic data is summarized below. The first stage involved removal of the relevant data from the TOBI data records. Conversion to pitch and roll in degrees and from pressure to depth in metres was accomplished at this point. Next, the data were subsampled at 2.5s intervals (to correspond to the gyro measurements) and the magnetometer manufacturer's calibrations were applied to convert to magnetic field in nT. Data spikes and time stamps were removed at this stage. The individual data files from the magneto-optical discs were then merged and subsampled into files corresponding to lines and turns, and position, based on Javier's TOBI navigation (see above), was added to the records, completing the initial level of processing.

The next stage of processing involved the application of a correction for the magnetic effect of the instrument, as detailed above, to give the corrected total field.

Formats and processing scheme for TOBI magnetic data

The following describes the **filenames** (in bold), `data formats` (in Courier) and *program names* (in italic) used in the on-board processing.

1) **cd99pN.mag** (where N is the number of the magneto-optical/laser disc).

```
Header        YYMMDD HHMM SSS     alt    wire    depth  Vx        Vy        Vz        roll   pitch
head
CD99 TOBI ru 960319 1923 190     486    3743    2180   132668    -32722    149954    0.78   -2.03
103.90
```

Note: SSS is seconds × 10 (e.g. 19 seconds). Depth is from pressure sensors, converted knowing the conductivity and temperature. Wire is wire-out, and is unreliable. alt is height above seafloor, picked from the vertical seismic profiler. This, too, is unreliable, as it relies on an automatic picking routine. Vx, Vy and Vz are the nominal voltages in the three-component magnetometer. These have to converted at a later stage into true voltages, and then into nT. The X magnetometer is horizontal, +ve to port, the Y is horizontal, +ve forward, and the Z is vertical, +ve down. Roll, pitch and head are measured in degrees, having been converted using the following corrections:

Pitch (deg) = reading/6.4 (+ve pitch is vehicle nose down).

Roll (deg) = reading/6.4 (+ve roll is vehicle down to starboard).

Data is at 0.5s. intervals.

⇓

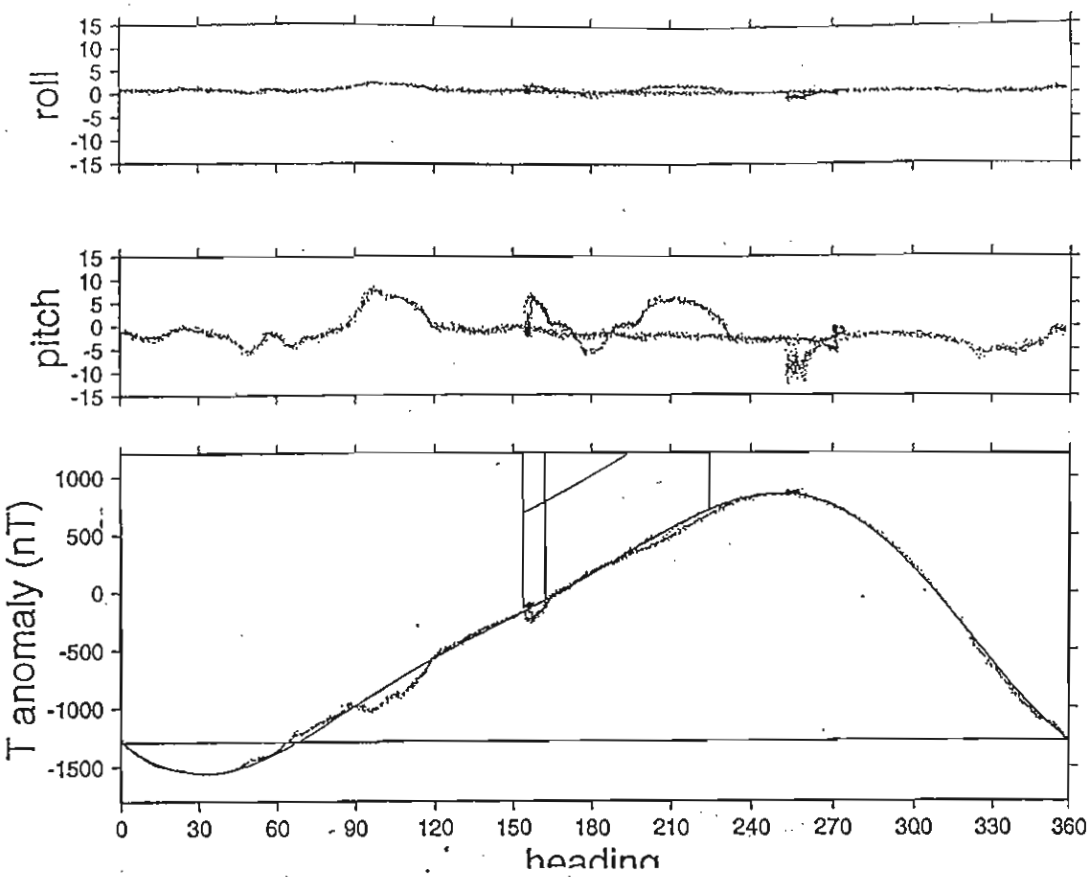

Figure 6: Total field after removal of IGRF & comparison with pitch and roll. Dots are obsevations, solid line is the Fourier fit in 5 terms and used as the heading correction.

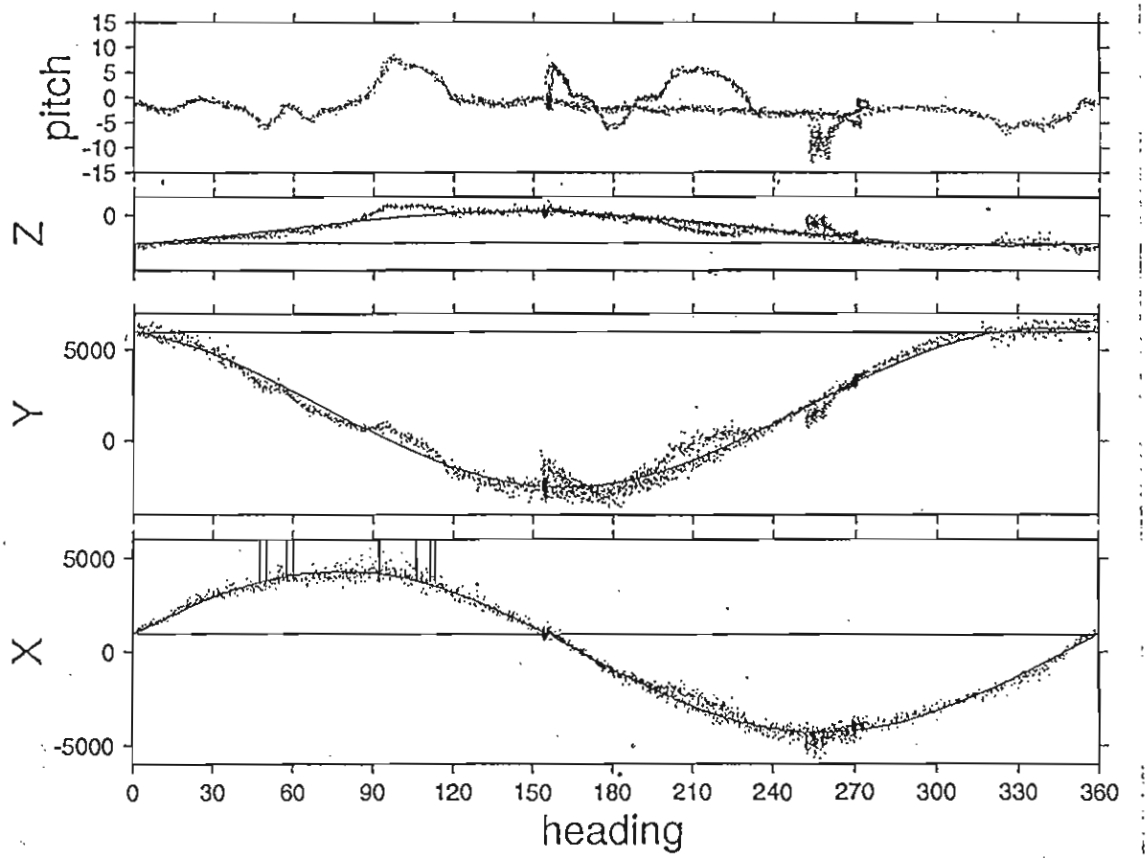

Figure 7: Three components with IGRF removed. Dots are observations, solid line is the Fourier fit in 3 terms and used as the heading correction.

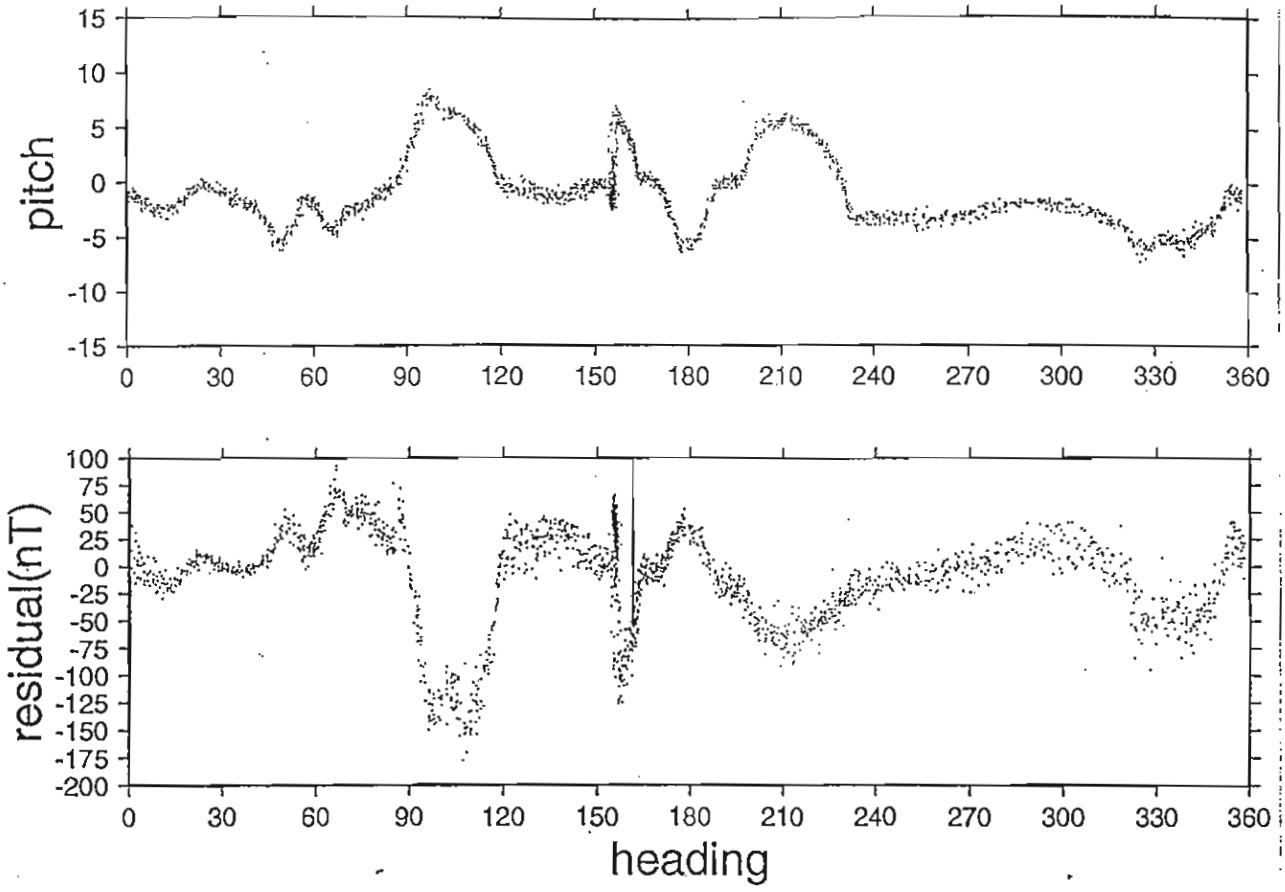

Figure 8: Total field residual after removal of theoretical Fourier model.

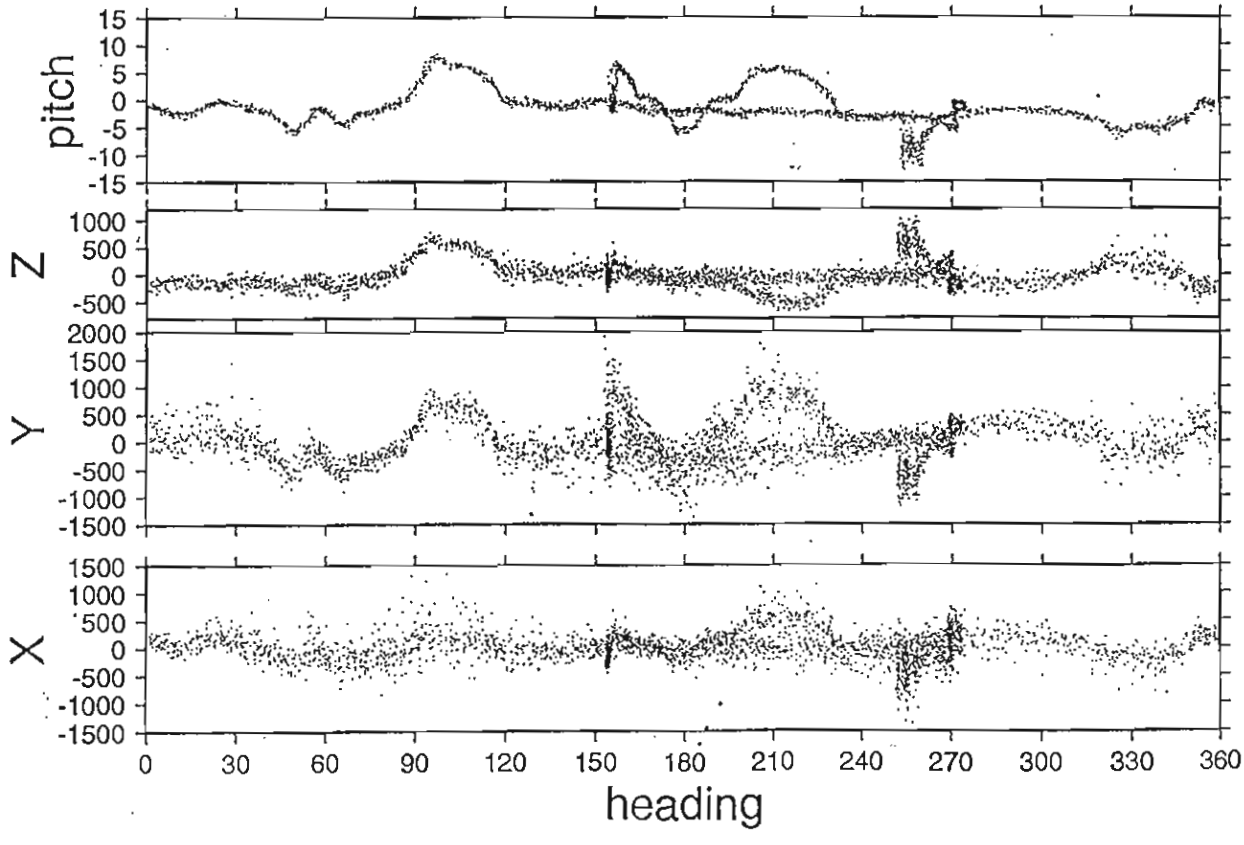

Figure 9: Residuals of the three components after removal of theoretical Fourier model.

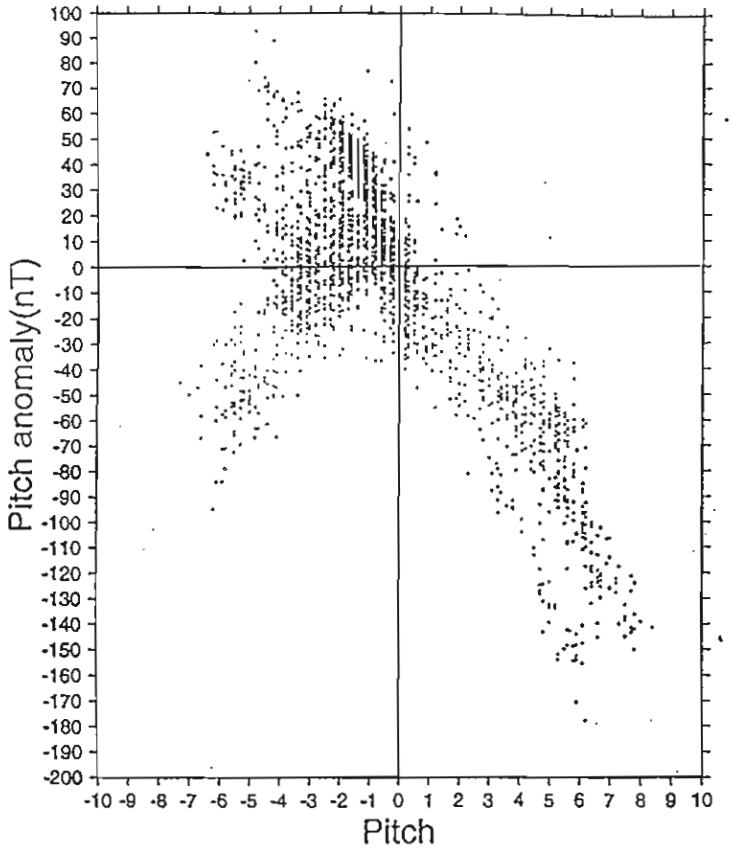

Figure 10: Pitch anomaly vs pitch for total field. Fairly linear!

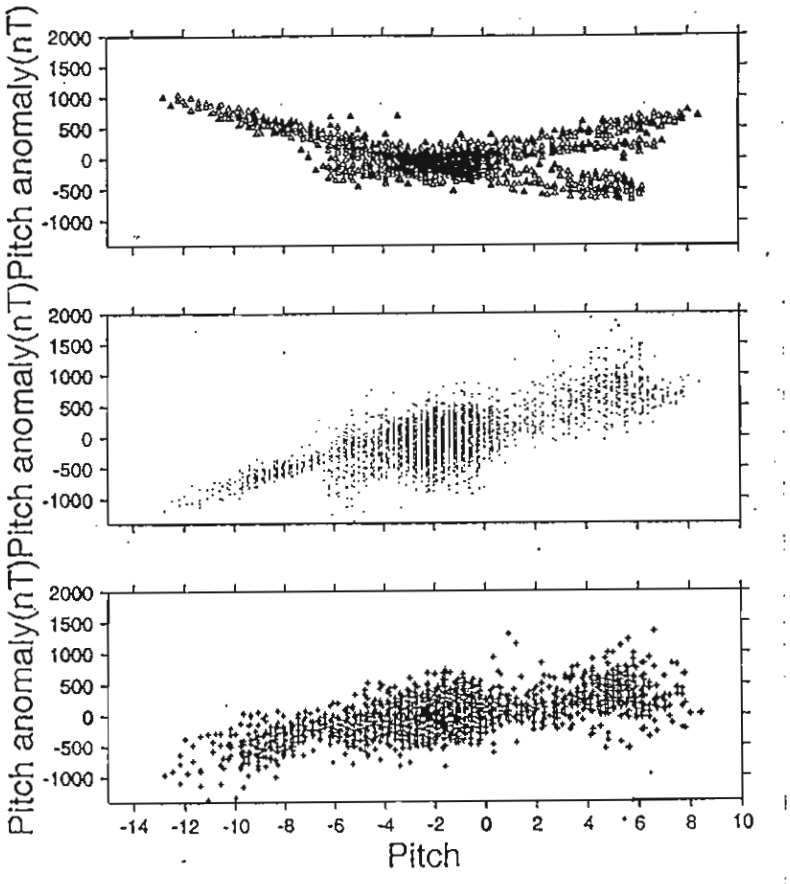

Figure 11: Pitch anomaly vs pitch for each of the three components. Crosses(bottom) for X, dots(middle) for Y, triangles(top) for Z.

⇓

promag2mat.auk

(converts to format readable in matlab)

⇓

2) **cd99pN.mat**

```
YYMMDD HHMM SSS Vx     Vy     Vz     roll pitch head   alt wire depth
960329 0843 040 111032 -78656 150603 1.09 0.47 128.90  988 1990 -3033
```

⇓

tomagcal3

(matlab routine, subsamples at 2.5s intervals, filters, applies magnetometer calibration, converts to nT)

This program selects data at 2.5s intervals (corresponding to gyro readings) and filters out time spikes and other bad data. It then converts from nominal volts to volts ($\times 2.5/2^{16}$), applies the manufacturers calibration to the data, and converts to nT (40 000nT/volt). The coordinate system is switched to X, horizontal, +ve forward; Y, horizontal, +ve starboard; and Z is vertical, +ve down. (Xmag = -Ytobi, Ymag = Xtobi, Zmag = Ztobi.). Output, to "cd99pN.nT" files, has the same general format as the "cd99pN.mat" files, but with vehicle coordinate magnetic fields in nT (Fx, Fy, Fz) substitued for Vx, Vy and Vz. tsec is the total time in seconds in 1996.

⇓

3) **cd99pN.nT**

```
YYMMDD  HHMM  SSS    , Fx       Fy       Fz      roll   pitch  head
alt  wire  depth   tsec
960320  1510    0     11285     29412     27306   1.88   5.47  287.90
970  2514  1855   6966600
```

⇓

getline

(matlab routine, gathers data for each line, adds navigation)

⇓

4) **line$_mag.nav** (where $ is the letter corresponding to the line)

```
YYMMDD  HHMM   SSS  Fx     Fy     Fz     roll   pitch  head    alt  wire
tsec     lat         lon          utmX       utmY
960320  1510   25  10948  29415  27439   1.72   4.84  287.70   970  2514
6966602 28.94950  -42.80133   714282.43  3204348.50
```

Lat and lon are in decimal degrees, utmX and utmY are in m (based on UTM84). TOBI navigation data are based on Javier's modelling.

⇓

total_field_corn

(fortran routine, applies correction for total field derived from "saftypin" correction, removes IGRF).

⇓

5) **line$.fx**

```
field   utmX         alt   depth  lat      lon
196.3   714282.438   970.  1856.  28.9495 -42.8013
```

Field is the total magnetics field anomaly in nT.

⇓

filter_mag

(matlab routine, filters data, adds bathymetry, subsamples at 100 m intervals along track)

The altitude selected is either a filtered form of the TOBI altitude, or the Simrad bathymetry - TOBI depth,
depending on which is least problematic.

⇓

6) **line$_mag.int**

```
utmX             field            depth            alt              lat
lon
7.1418244e+05    1.9294373e+02    1.8719233e+03    8.8897921e+02
2.8949500e+01   -4.2802395e+01
```

⇓

invert_mag

(applies Parker and Huestis inversion to deep-towed data)

⇓

⇓

7) **line$.inv**

```
 magnetization  recomputed field  annihilator    utmX            alt
depth
 1.5014608e+00   5.2223015e+01   1.2306528e+00   8.1400000e+01   -
9.7210217e-01  -2.5751022e+00
```

Magnetization in A/m, recomputed field in nT, annihilator in A/m, utmX, alt and depth in km.

Preliminary results

Total magnetic field data

Initially, we combined the three-component TOBI data to give the total field (Figure 12). The deep-towed magnetic measurements contain much greater structure than the corresponding surface records. Wavelengths are dependent on depth, but are faithfully recorded down to about 500 m. Amplitudes are recorded in excess of 4000 nT peak-to-trough. The field generally defines a central high along the axial valley within the Bruhnes. The Matuyama and Gilbert can tentatively be identified, out to about 30 km from the axis. The magnitude of the central anomaly high increases from the north to the south along the axis.

Inversion to magnetization.

We have used the Parker and Huestis (1974) inversion for magnetization from total field, using the altitude of TOBI above the sea floor, making the assumption of Hussenoeder et al. (1995), that the vertical gradients of the TOBI track are relatively low. This method is preferred over upward continuation to a common datum, as high wavenumber elements of the data are inevitably reduced in this process.

The altitude of TOBI was determined in two ways; from the vertical seismic profiler, and from subtracting the TOBI depth (measured from a pressure sensor) from the Simrad centrebeam bathymetry. We have compared the profiles from the different methods and chosen which to use on the basis of which provided the best representation of the bathymetry. The seismic profiler altitude data were initially filtered using a simple boxcar filter applied in the Fourier domain.The data were subsampled at 100 m intervals, which was sufficient to record the high wavenumber component of the signal. The assumed thickess of the magnetized layer was 0.5 km, and the high-pass filter was 1 km.

The inversion was generally successful in modelling the character of the anomalies, including the short wavelength components (Figure 13). The first stage of the inversion involves the removal of any linear trend in the data, which caused problems with some of the shorter profiles, such as line R, and interrupted profiles, such as line J, because removal of the linear trend has removed the central anomaly. Lines U and V, which run parallel to the strike of the anomalies were not inverted.

The magnetization determined by the inversion shows a distinct variation along the strike of the axis. In the north the central high within in Bruhnes is relatively subdued, whilst in the south it is characterised by an asymmetric region of high magnetization. Some individual volcanic features appear to correspond to large magnetic anomalies and to high magnetizations. For example, the large anomaly on line Q occurs over Sumpter seamount.

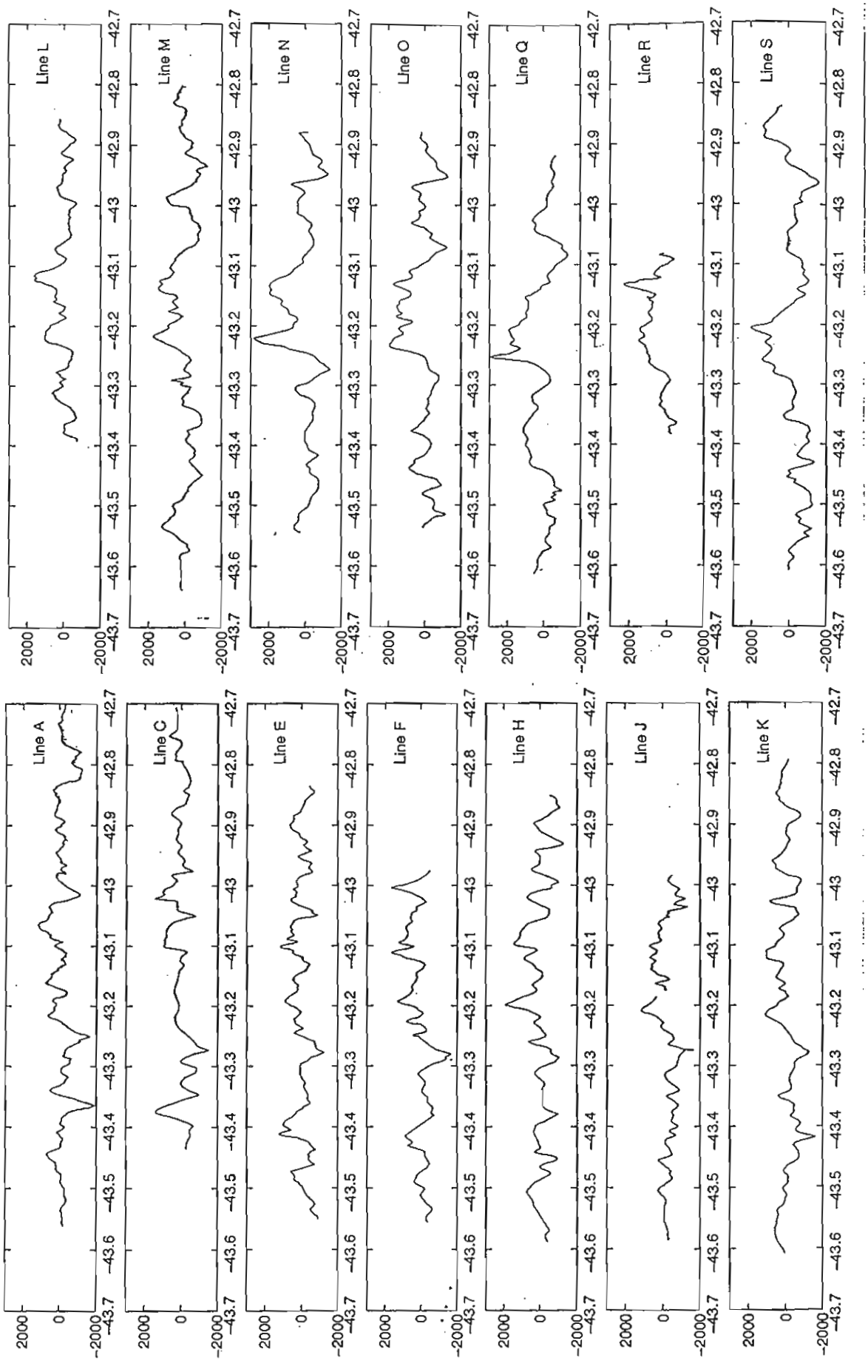

Figure 12: Total magnetic field measured by TOBI along the 14 E-W survey lines processed. on board. See Figure 2 for profile locations.

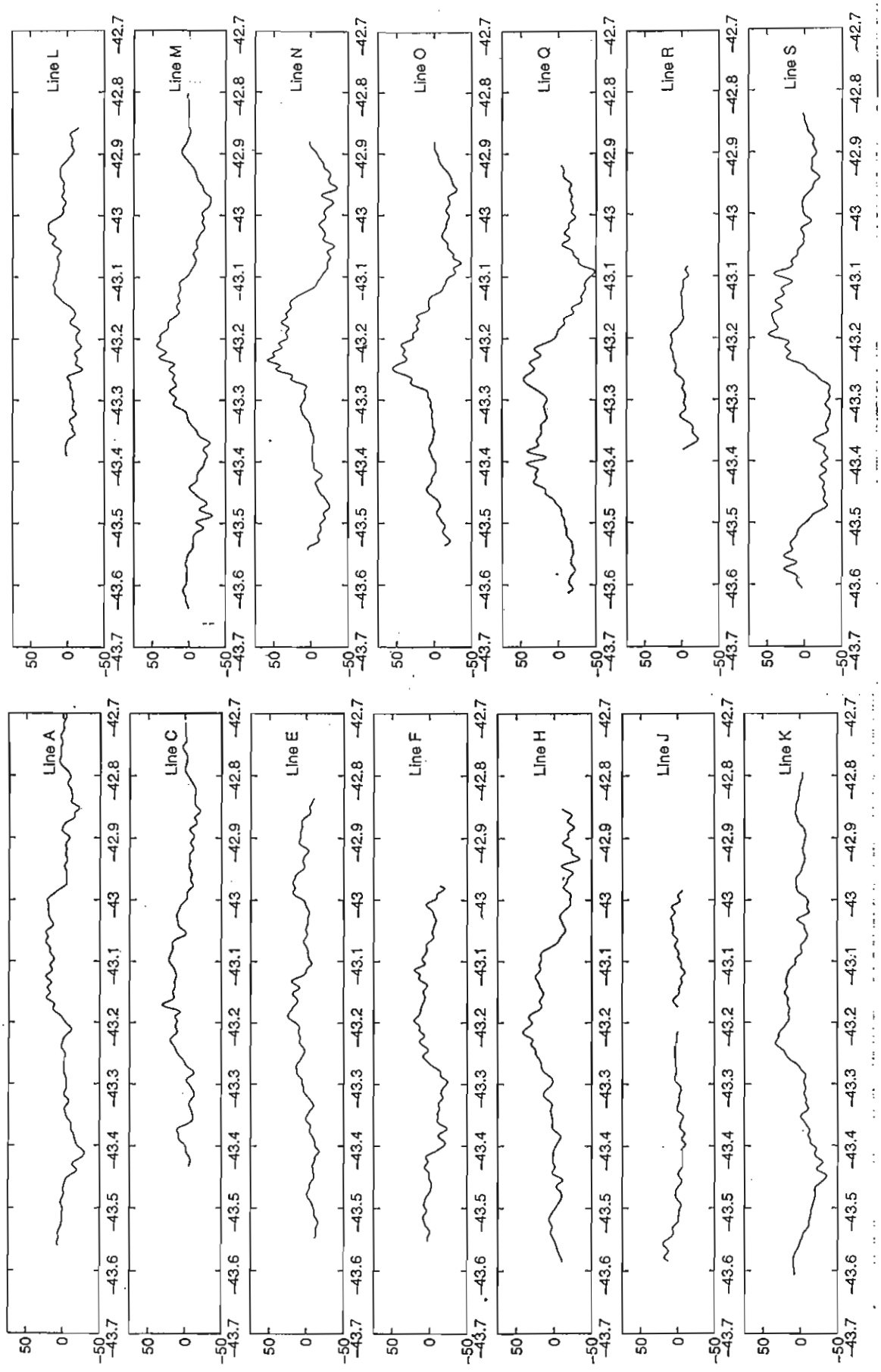

Figure 13: Crustal magnetzation deduced from TOBI total magnetic field, assuming a 0.5 km thick crust. See Figure 2 for profile locations.

Shipboard Three-Component Magnetometer (STCM)

(Tomoko Tanaka)

Introduction

Vector data of the geomagnetic field were collected with the Shipboard Three Component Magnetometer (STCM) during this cruise. The vector magnetic data provide more detailed information than total intensity data to understand the magnetic structure of oceanic crust, because the amplitude of vector magnetic anomalies are not affected by the direction of the ambient geomagnetic field or the strike of magnetic lineations. The STCM system has been developed and improved since 1977 (Isezaki et al., 1981; Seama et al., 1990). It has been used in many oceanic regions to successfully measure the geomagnetic field vector (e.g. Seama and Isezaki 1990; Nogi et al., 1990; Seama et al., 1993). The geomagnetic fields observed by the STCM are superimposed on the magnetic field produced by the induced and permanent magnetic moments of the ship. The ambient geomagnetic field vector is calculated by reducing those artificial magnetic fields. For this calibration, we steered the ship in "figures of eight" at 8 sites.

Instrument and Data Acquisition

The STCM consists of a flux-gate magnetometer, two gyro-compasses, and a personal computer. The sensors of the magnetometer consist of three axial flux-gate coils. The sensor package was rigidly mounted on the starboard side of the main mast cross-tree. Since this was relatively close to the midships gantry, care was taken to ensure that the latter was fully retracted to the same position at the end of each station operation. All of the other instruments were installed in the Main Laboratory. The flux-gate magnetometer measures individual x, y, and z components of the magnetic field. The gyro-compasses obtain the ship's yaw, pitch and roll data. These data are transferred to a personal computer.

In this cruise, the STCM was not linked directly to the ship's navigation and geophysical data acquisition system (which provides the ship's position, yaw, water depth, and magnetic total intensity data obtained by the proton precession magnetometer), but we obtained these data by network file transfer and then combined them with the STCM data. Due to problems with the magnetometer gyro, all the processing was done using the ship's gyro data.

Sample Data

X, Y, and Z indicate the northward, eastward and downward components of the vector geomagnetic anomalies, respectively. Data for selected E-W lines are shown on Figure 14. The measured data were corrected for roll, pitch, yaw, and ship's induced magnetic field using the 12 calibration constants (Table 1) derived from seven of the STCM calibration sites R1-R7 (Table 2) using the method of Isezaki (1986). To obtain the magnetic anomaly we subtracted the field predicted by IGRF90 from that measured.

Table 1: List of '12 Constants'

0.98774	-0.39561	-0.39561	-6146.2
0.42693	1.06775	1.06775	-2289.4
-0.01319	0.05253	0.57325	3194.2

Table 2: STCM Calibration Sites

Site	Date	Time start	Time end	Latitude	Longitude
R1	07 Mar.96	09:02	09:21	33° 06.4'N	26° 06.8'W
R2	10 Mar.96	09:43	09:57	31° 06.1'N	34° 46.0'W
R3	10 Mar.96	09:58	10:44	31° 06.0'N	34° 46.0'W
R4	12 Mar.96	09:49	10:07	29° 00.2'N	43° 19.1'W
R5	12 Mar.96	10:07	10:27	29° 00.6'N	43° 19.2'W
R6	14 Mar.96	10:58	11:17	28° 49.7'N	43° 38.5'W
R7	14 Mar.96	11:25	11:47	28° 50.4'N	43° 40.1'W
R8	15 Mar.96	09:20	09:40	28° 57.0'N	43° 21.0'W

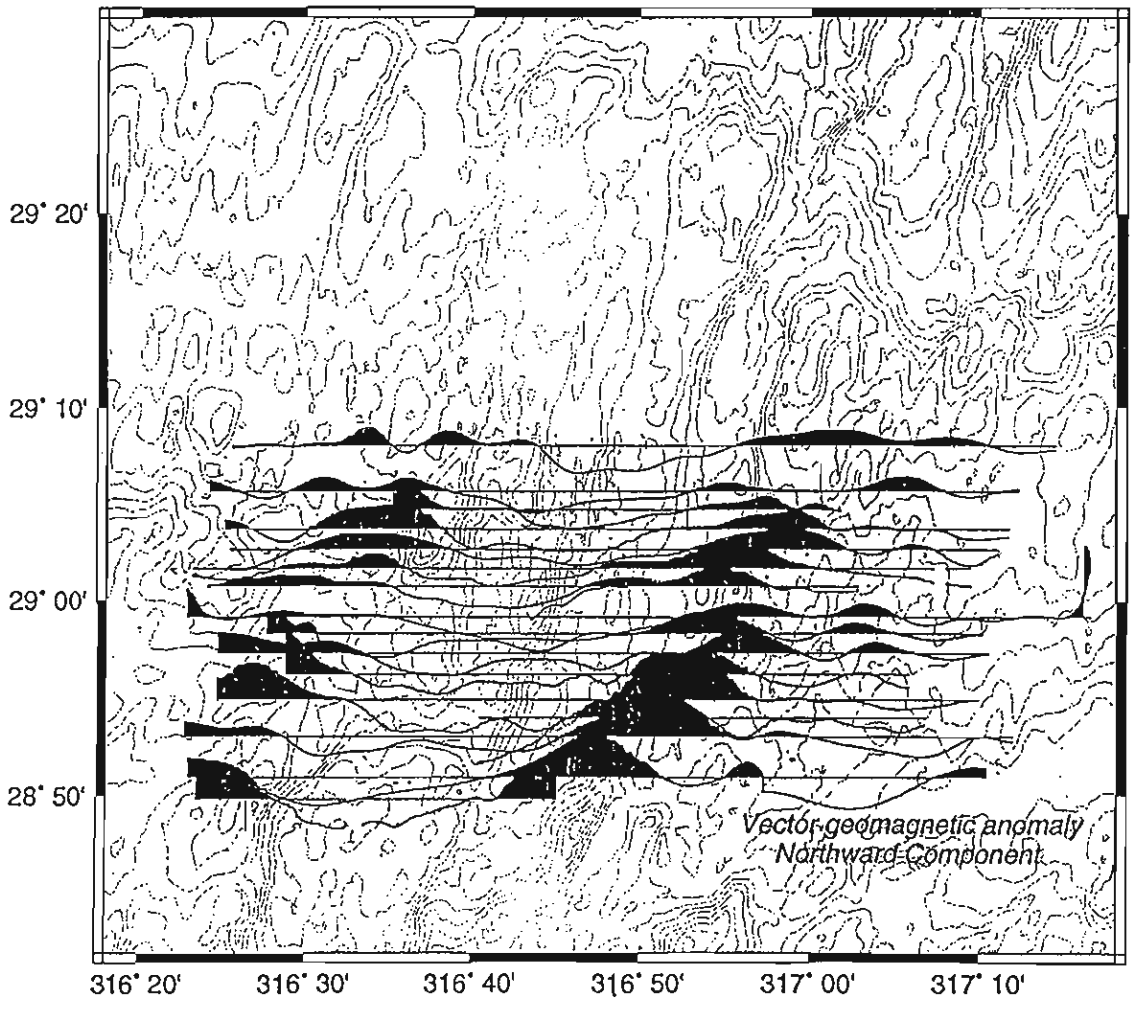

Figure 14a: Vector geomagnetic anomalies obtained from the shipboard three-component magnetometer: north component (X)

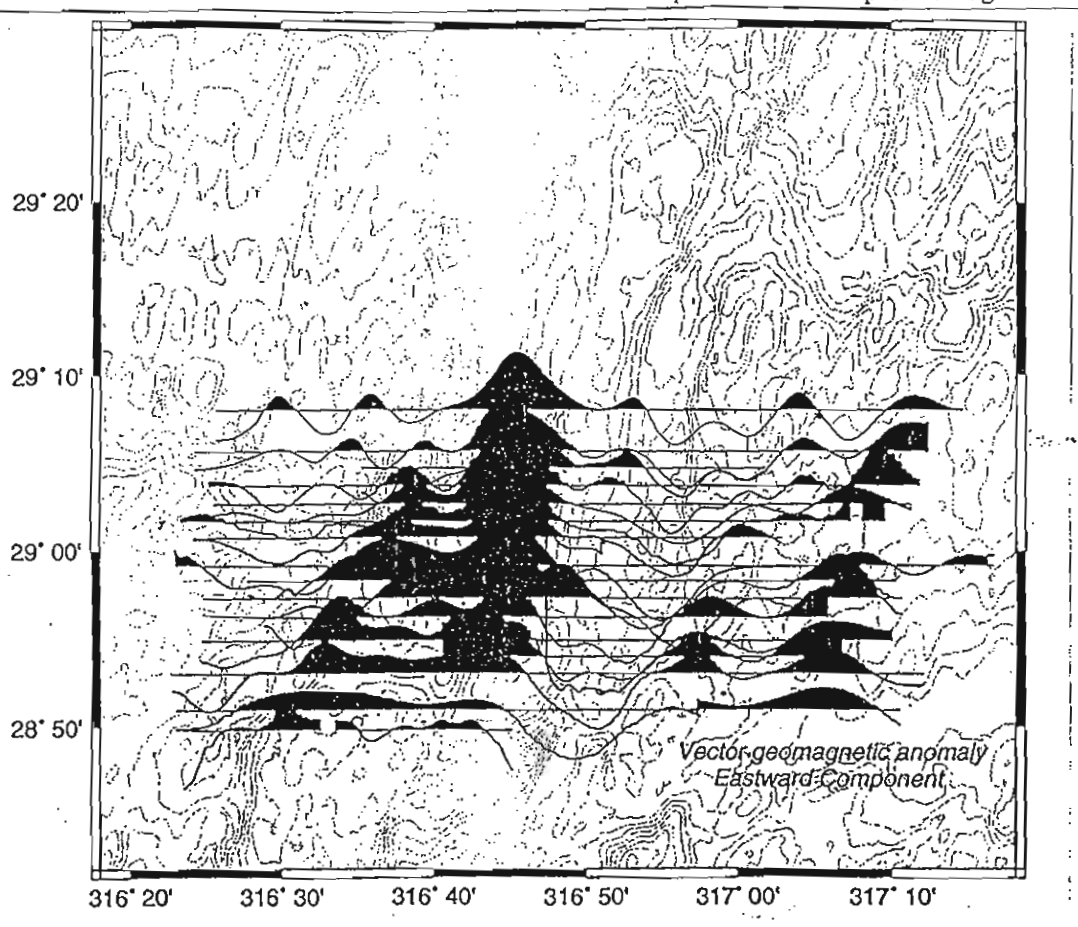

Figure 14b: Vector geomagnetic anomalies obtained from the shipboard three-component magnetometer: east component (Y)

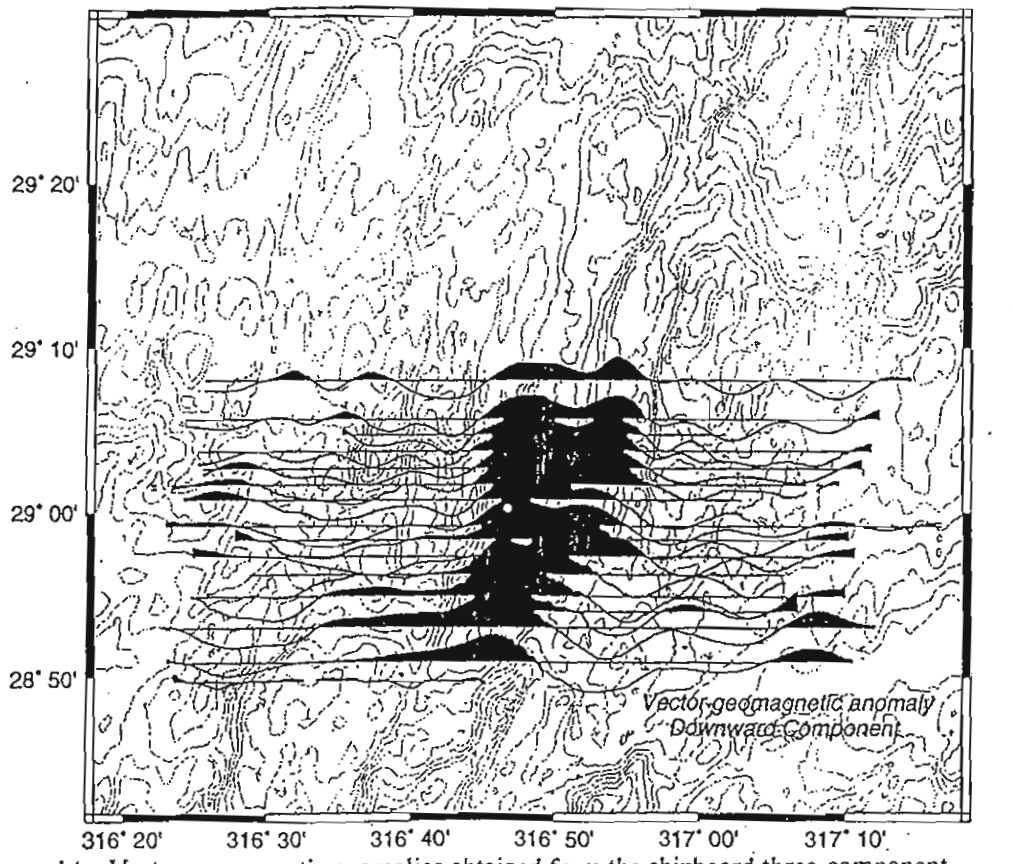

Figure 14c: Vector geomagnetic anomalies obtained from the shipboard three-component magnetometer: vertically down component (Z).

Dredge Stations

(Chris MacLeod)

Seven dredge stations were attempted on this cruise (Figure 15). All but one (D6) were successful. In each case we deployed a standard rectangular frame dredge with chain-link bag and net liner, with a cylindrical steel pipe dredge towed a short distance behind. A length of chain preceded the dredge, and a pinger was placed on the wire 100 - 200 m above the dredge. The results are described below.

CD99 D1

12th March 1996: 28° 55.6'N 43° 14.1' W

Objective: High magnetisation region of the axial valley coincident with the axial volcanic ridge at the southern tip of the Broken Spur segment.

	Time	Lat	Long	Depth	Wire out
Deployment	1306	28° 55.4'N	43° 14.3' W		
On bottom 3568m	1442	28° 55.6'N	43° 14.1' W	3536m	
Off bottom 3562m	1511	28° 55.6'N	43° 13.7' W	3432m	
Recovery	1629	28° 55.6'N	43° 13.3' W		

Recovery: slightly to moderately altered glassy pillow rinds (some striae on outer surfaces).
Size distribution: 5-10cm: 5 pieces; 2-5cm: 11 pieces; <2cm: ~40 pieces.
Lithology: glassy to fine-grained, dark grey to black heavily plagioclase-phyric basalt. Proportion of phenocrysts up to ~30%. Plagioclase phenocrysts typically in size range 1mm to 4mm; some megacrysts up to 12mm long.
Alteration: outer (convex) surfaces of pillow rinds have rust-coloured surface ~ 1mm thick, often over a white clay alteration, and locally covered by a thin, black (?Mn) surface alteration. Inner surfaces are often partially covered by a light cream clay alteration (or possibly traces of pelagic sediment; locally also Mn coat. Some of the small pieces show very little evidence for alteration - fresh or only slightly devitrified black glass.
Biology: one piece has a fine, white, soft, mesh-textured crystalline (siliceous?) growth on surface, over the alteration surface, interpreted as a deep-water sponge or possibly an algal structure or coral.

CD99 D2

13th March 1996: 28° 54.4'N 43° 14.6' W

Objective: High magnetisation region of the axial valley coincident with the axial volcanic ridge at the southern tip of the Broken Spur segment.

	Time	Lat	Long	Depth	Wire out
Deployment	0907	28° 54.5'N	43° 14.8' W		
On bottom 3600m	1039	28° 54.4'N	43° 14.6' W	3587m	
Off bottom 3580m	1215	28° 54.9'N	43° 13.8' W	3617m	
Recovery	1342	28° 55.3'N	43° 12.7' W		

Recovery: (in pipe dredge) slightly to moderately altered glassy basalts, some clearly pillowed (some growth striae on outer surfaces), contained in sticky pale brown pelagic sediment.

Size distribution: 10-20cm: 4 pieces, 5-10cm: 7 pieces; 2-5cm: ~60 pieces; <2cm: ~2kg. Pelagic sediment: ~10kg (~0.5kg sampled).
Lithology: glassy to fine-grained, grey to black aphyric basalt, with spherules and very small (<0.5mm) sparse vesicles.
Alteration: Extremely fresh, with little evidence of alteration. Some have minor amounts of rust-coloured alteration on the surface.
Sediment: Large amount of buff, pale cream, pelagic sediment.
Biology: strange branching stick-like growth approx. 20cm high. Tubes 0.5-1cm diameter, of white ?calcite with a central tube. Broad flat base approx 10cm diameter adhering strongly to pillow lava surface (glass brought up with base). Patches of dark brown-black surface coat adhere to tubes and (especially) to base.

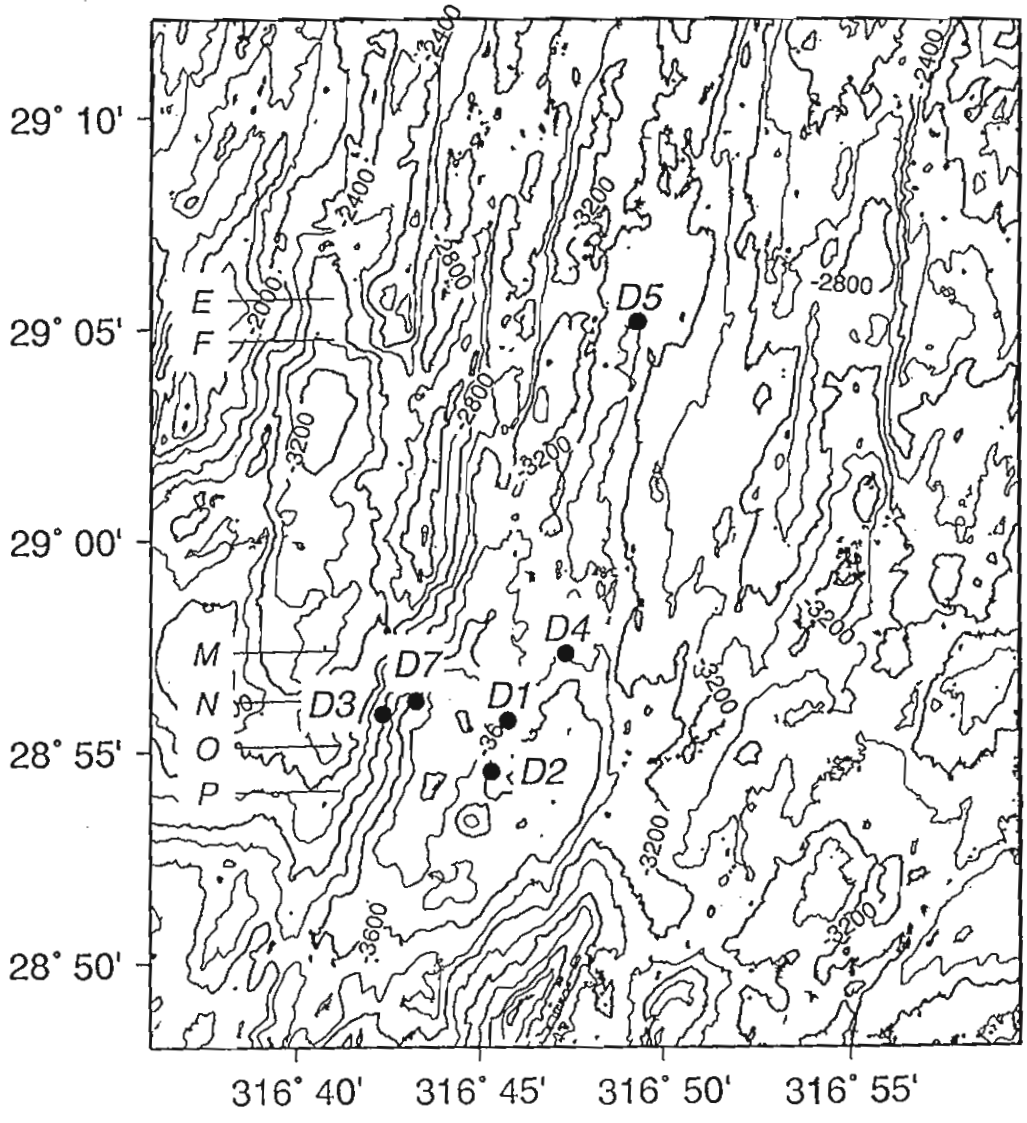

Figure 15: Locations of dredge stations (dots). Letters indicate the latitudes of the neighbouring TOBI lines.

CD99 D3
13th March 1996: 28° 55.8'N 43° 17.5' W
Objective: Inside corner fault scarp at southern end of Broken Spur segment, very close to the reported location of serpentinite debris flow recovered by CD65 dredge RD34 (given as 28°55.2'N, 43°17.39'W in CD65 cruise report). The intention was to dredge the very steep slope interpreted as the footwall of the fault scarp above the talus fan to see if gabbros and peridotites crop out there, and thence to test Joe Cann's hypothesis that the serpentinite protruded up the fault.

	Time	Lat	Long	Depth	Wire out
Deployment	1459	28° 55.8'N	43° 17.5'W		
On bottom 3028m	1638	28° 55.84'N	43° 17.92'W	2896m	
Off bottom 2745m	1744	28° 56.30'N	43° 18.43'W	2646m	
Recovery	1840	28° 56.4'N	43° 18.0' W		

Recovery: >250kg of heavily to very heavily altered pillowed basalt debris with rare indurated cataclasite blocks, fault breccia and buff-coloured pelagic mud.

Unit 1: Altered pillow basalt.
Size distribution: probably in excess of 2000 pieces in total. Largest blocks 30 x 30 x 20cm.
Lithology: aphyric basalt, glassy to medium-grained (acicular plagioclase laths in holocrystalline pillow interiors up to a couple of mm long); usually vesicular. Vesicles usually very small (<1mm) but some up to 6-7mm, never filled but often lined by brown Fe-oxides and/or black Mn oxide. All material apparently of extrusive origin, from form of blocks, presence of vesicles and grade of alteration.
Alteration: blocks covered by variable degree of black Mn- or orange Fe-oxide coating or (more often) by pale grey to buff clay-grade alteration. Blocks may be covered on all sides (implying already broken and weathered on seafloor, not plucked from bare-rock outcrop). Most lava weathered to pale grey colour on all surfaces; when broken is darker grey in fresher core. Some fragments of slightly altered glass preserved on outer rims of pillows. Devitrification spherules visible within a few cm of pillow margin, coalescing towards holocrystalline centre of pillow. Several of the larger lava fragments tougher, apparently more heavily altered, with larger vugs lined with orange (haematite-stained) ?zeolite crystals, and possibly some mineral precipitated in the groundmass to give the blocks their extra hardness.

Unit 2: ?Cataclasite
Size distribution: 10 - 20cm: 1 piece; 5-10cm: 2 pieces; 2-5cm; 7 pieces.
Lithology: lithified blocks of fine-grained, indurated white to buff rock, containing lots of small (<1mm) angular fragments of black lava. The white material often forms a matrix to a matrix-supported breccia, the clasts being irregular blocks of altered lava debris. These surfaces are in most instances covered by slickensides. No microfossils are observed in hand-specimen. We provisionally interpret these rocks as indurated rock-flour resulting from cataclasis, though it is possible that they may be indurated pelagic sediments that contain fragments of lava and have been incorporated into the fault zone.
Alteration: the rocks are mostly part-covered by black Mn staining.

Unit 3: Fault breccia
Size distribution: 5-10 cm: 1 piece.
Lithology: light green-grey matrix-supported monomict breccia, comprised of angular, polished clasts of grey-green lava. Clast surfaces are polished and striated, but no visible fabric is evident. The largest clasts are ~0.5 cm in diameter. This rock is interpreted as an indurated fault breccia.
Alteration: rust-coloured alteration affects the outer 2mm.

Unit 4: Pelagic mud
Lithology: pale cream- to buff-coloured fine-grained pelagic sediment.

Biology: curved white ?calcareous worm casts, (<1mm wide, up to 2cm long) on altered lava blocks very common. In pipe dredge rock fragments covered by very large numbers of small white delicate shelled creatures (<1cm) with a variety of shapes: many tapering elongate cones or open-ended cylinders; others triangular with swollen centres (with delicate spines); others have the form of spiral, flat discs; possibly large coccoliths.

CD99 D4

15th March 1996: 28° 57.2'N 43° 12.5' W
Objective: Moderate magnetisation region of the axial valley east of the axial volcanic ridge at the southern tip of the Broken Spur segment.

	Time	Lat	Long	Depth	Wire out
Deployment	1115	28° 57.2'N	43° 12.5' W		
On bottom 3548m	1251	28° 57.2'N	43° 12.5' W	3502m	
Off bottom 3374m	1405	28° 56.9'N	43° 11.7' W	3407m	
Recovery	1514	28° 56.5'N	43° 10.9' W		

Recovery: slightly to moderately altered glassy pillow lavas.
Size distribution: 20-50cm: 25 pieces; 10-20cm: 40 pieces; <10cm: ~200 pieces.
Lithology: dark grey-black aphyric pillow lavas, fairly fresh glass at margins. Some microvesicles, and vuggy regions (irregular interconnected voids up to ~ 1cm in diameter).
Alteration: Vuggy areas are often infilled with zeolite (often oxide-stained). Some Mn staining on joint surfaces of pillow blocks, elsewhere tiny spots of black Mn common on the surface of joint faces.
Sediment: More than 10 kg of buff-pale cream pelagic sediment recoved; ~ 0.5 kg retained.

CD99 D5

15th March 1996: 29° 05.0'N 43° 10.4' W
Objective: Low magnetisation region of the axial valley east of the axial volcanic ridge at the centre of the Broken Spur segment.

	Time	Lat	Long	Depth	Wire out
Deployment	1630	29° 05.0'N	43° 10.4' W		
On bottom 3392m	1740	29° 04.9'N	43° 10.3' W	3416m	
Off bottom 3387m	1832	29° 04.5'N	43° 09.8' W	3335m	
Recovery	1945	29° 04.0'N	43° 09.3' W		

Recovery: slightly to moderately altered glassy pillow lavas.
Size distribution: 20-50cm: 1; 10-20cm: 13; 5-10cm: 5 pieces; <5cm: 50 pieces plus several kg of rubble.
Lithology: glassy to fine-grained, grey-black aphyric or very sparsely plagioclase phyric ± olivine phyic basalt. A few pieces are heavily plagioclase phyric. Those pieces are moderately plagioclase phyric, with rare green olivine phenocrysts. Plagioclase phenocrysts are up to ~5mm, mostly 1-2mm. Olivine 1-2mm. Total phenocrysts ~10-15%.
Alteration: some Mn and yellow-buff alteration on joint surfaces of pillows.
Sediment: cream - buff pelagic sediment. More than 20 kg recovered; 0.5 kg retained.

CD99 D6

29-30th. March 1996: 28° 56.03'N 43° 16.45'W (projected start)
28° 56.20'N 43° 16.65'W (projected end)

Objective: To dredge outcrops (in between talus fans) on lowermost slopes of large fault scarp at inside corner at SW end of 29°N segment, to see if peridotites and/or gabbros are exposed there.

	Time	Lat	Long	Depth	Wire out
Deployment	2239*	28° 56.04'N	43° 16.29'W		
On bottom 3852m	0022	28° 56.11'N	43° 16.59'W	3607m	
(9-ton pull 3722m)	0135	28° 56.62'N	43° 17.11'W	3225m	
Off bottom 3283m	0200	28° 56.87'N	43° 17.23'W	3143m	
Recovery	0310	28° 57.23'N	43° 17.61'W		

*29th. March 1996

Recovery: none. Dredge lost.

CD99 D7

30th. March 1996: 28° 56.07'N 43° 16.50'W (projected start)
28° 56.20'N 43° 16.65'W (projected end)

Objective: To dredge outcrops (in between talus fans) on lowermost slopes of large fault scarp at inside corner at SW end of 29°N segment, to see if peridotites and/or gabbros are exposed there.

	Time	Lat	Long	Depth	Wire out
Deployment	0356	28° 56.06'N	43° 16.49'W		
On bottom 3799m	0525	28° 56.18'N	43° 16.51'W	3600m	
Off bottom	0624	28° 57.02'N	43° 17.14'W	~3010m 3370m	
Recovery	0730	28° 57.72'N	43° 18.17'W		

Recovery: ~150kg of slightly to very heavily altered aphyric and plagioclase-phyric pillow lava debris, plus a few blocks of coarser-grained dolerite (from massive flows or possibly dyke rock), two pieces of coarse-grained gabbro, and one piece of indurated buff-coloured sediment.

Unit 1: Altered pillow lava
Size distribution: several hundred pieces in total. Largest blocks pillows up to 30 x 30 x 30cm. Approximately 70% of samples aphyric, 30% plagioclase-phyric.
Lithology: (1) aphyric pillowed basalt, glassy to spherulitic and thence fine-grained (acicular plagioclase laths in holocrystalline pillow interiors up to a couple of mm long). Lava usually vesicular, with most vesicles very small (<1mm) but some up to 6-7mm; these are not filled but often lined by brown Fe-oxides and/or black Mn oxide. Grain size of most internal portions of pillows (approx. 25cm from margin in largest samples) still very fine (though holocrystalline): acicular plagioclase crystals estimated at <2-3mm long by 0.1-0.2mm wide. Glassy rinds up to 0.5cm thick are preserved on a few otherwise altered-looking pillow margins, and a few pieces of very fresh-looking aphyric vitreous glass up to 1cm3 were recovered. (2) moderately to heavily plagioclase-phyric pillowed basalt (with a few percent olivine in addition in a few samples); appearance otherwise as above. Proportion of phenocrysts is variable, and apparently greatest (at ~15%) at (upper?) margins of pillows. Plagioclase phenocrysts are euhedral to subhedral, up to ~1cm long at maximum, with aspect ratios ranging from 1:1 to 1:3.

Alteration: orange palagonite after glass on margins of most pillow fragments. Thin coating of very fine ?clay alteration on block margins, on what would have been internal radial cracks of pillows. Other blocks are covered by a variable degree of black Mn- or orange Fe-oxide coating or (more often) by pale grey to buff clay-grade alteration. Some blocks are covered on all sides (implying already broken and weathered on seafloor, not plucked from bare-rock outcrop). Most lava weathered to pale grey colour on all surfaces; when broken is darker grey in fresher core (this material may be very fresh). Devitrification spherules visible within a few cm of pillow margin, coalescing towards holocrystalline centre of pillow. Several of the larger lava fragments tougher, apparently more heavily altered, with larger vugs lined with orange (haematite-stained) ?zeolite crystals, and possibly some mineral precipitated in the groundmass to give the blocks their extra hardness. One sample has pearly white coloured zeolite (analcime/heulandite?) on surfaces next to a vuggy patch.

Unit 2: Massive lava
Size distribution: 20-50cm: 1 piece; <20cm: approx a dozen pieces.
Lithology: light grey, fine- to medium-grained holocrystalline basalt/dolerite, usually aphyric but very rarely with plagioclase phenocrysts up to 1cm in length. It is usually microvesicular, with a few percent empty spherical vesicles <1mm in diameter. Groundmass plagioclase is acicular, up to 3-4mm x 0.5mm in size, with typical random interlocking texture. One block of massive lava has two parallel surfaces and traces of a glassy margin on (the top) one, and has well-developed columnar jointing perpendicular to these surfaces. This almost certainly comes from the top of a sheet flow. Other blocks are bounded by joints on all surfaces and have no chills of any kind; these may either be from the internal portions of flows or from dykes. An origin in the sheeted dyke complex is possible, but thought less likely than an extrusive origin because of the presence of vesicles and from the apparent low grade of alteration (see below; N.B. this will have to be verified post-cruise).
Alteration: samples may superficially be quite soft and green, though when hammered open several samples were found to have a fresh grey crystalline core. Most blocks are covered by a variable degree of black Mn- or orange Fe-oxide coating or pale grey to buff clay-grade alteration. Some blocks are covered on all sides, implying the dredged blocks were already broken and weathered on seafloor, not plucked from bare-rock outcrop.

Unit 3: Hyaloclastite breccia
Size distribution: 5-10 cm: 2-3 pieces.
Lithology: extremely soft and friable green breccia, consisting of altered glass fragments a few mm in size in a green matrix. No polishing or striation of clasts is evident. This rock is thought most likely to be an altered hyaloclastite breccia, though it is conceivable that it may be a fault gouge.

Unit 4: Gabbro
Size distribution: 2 pieces: one 12 x 8 x 8cm, the other 8 x 6 x 5cm with slickensides on one surface.
Lithology: Very coarse-grained isotropic gabbro. Equant interlocking crystals of clinopyroxene and plagioclase up to 1.5cm in size. Smaller rounded pits with fine mesh of magnetite are very probably pseudomorphs after olivine chadacrysts. There is no macroscopic sign of any shape fabric or crystal deformation. The smaller sample has one smooth surface covered by a dark green fine-grained mineral with striations, almost certainly either chlorite or actinolite. This dark green mineral may be up to 1-2mm thick, with a possible vague foliation parallel to the striated surface, implying that it may possibly be a fine-grained fault rock (either an ultramylonite or ultracataclasite) rather than simply a brittlely-sheared hydrothermal vein.
Alteration: Both pieces are slightly weathered, but are quite angular. The larger piece has some patchy dark surfaces but it is not obvious whether this is Mn staining or alteration of crystals; the smaller piece has traces of buff-coloured material (pelagic sediment?) in some crevices. Two thin parallel, planar hydrothermal veins (<0.5mm wide) are present in the larger sample; they contain an opaque white mineral that may be prehnite or something similar.

Unit 5: Lithified sediment
Size distribution: 1 piece, approx 15 x 10 x 5cm.
Lithology: pale buff-coloured fine-grained indurated sediment with black Mn-oxide coating. Contains isolated fragments of slightly altered (still vitreous) glass, brown Fe-oxide-rich specks and white spherules up to 1-2mm diameter (possibly foraminifera?). Could conceivably be completely

propylitised lava or indurated fault rock, but is thought unlikely (cf. similar samples with slickensides in dredge #3).

Biology: rare curved white ?calcareous worm casts, (<1mm wide, up to 2cm long) on altered lava blocks. One white, finely crystalline siliceous patch approx. 8mm diameter, with partially interwoven mat of spicular needles radiating away from small central hole ~1mm in diameter.

SHRIMP (Seabed High Resolution IMaging Platform)

(David Edge)

Due to the limited development phase of SHRIMP, facilities for this cruise were limited to photographic reconnaissance only. The equipment provided comprised a robust stainless steel framed vehicle (3m x 1m x 1m) with a *SOC-OTD* 10 kHz acoustic telemetry unit, *Simrad Mesotech* 200 khz altimeter, two *Deep Sea Power & Light* 12 V pressure balanced batteries, *Ocean Instrumentation* photographic camera and 1200 J flash unit. The shipborne control unit comprised a cabinet mounted PC operating line-scan waterfall display software and equipped with an internal A/D card . The PC was connected to a rack-mounted interface unit which provided a 24 V battery charger, 10 khz receiver and signal generator. Acoustic signals were received from the RVS PES towed fish. An RVS *Waverley* (now *Dowty*) thermal line-scan recorder provided a hard copy output.

Experiences obtained on CD95 showed that mid-ships operation of the vehicle provided the most stable position. The effect of ship's heave is significantly reduced which assists deployment and operating the vehicle close to the seabed. The camera is activated by the acoustic telemeter when the altimeter indicates an altitude of less than 10 m. Within this range the camera operates at a pre-selectable repetition rate. The camera has a film capacity of up to 1850 full frames.

Kodak 5297 colour high speed negative film was to be used for all operations except for the initial deployment, where Kodak Tmax 400 black & white negative film was used. Capabilities for onboard development of the latter would confirm correct camera and flash operation.

Shortly after the first deployment the acoustic telemeter stopped transmitting. On recovery the unit was found flooded. The unit was stripped down and all electronics cleaned. All 'O' seals were inspected but nothing obvious was found. The unit was reassembled with new seals and wire-tested to 3500 m. The problem did not recur.

Prior to the second deployment the flash unit failed to operate. The acoustic telemeter was designed to operate the camera twice after turning on, irrespective of the altimeter value. This provides a check that all is functional. On inspection of the camera it was found that the film advance mode was incorrect. After each operation the film should advance one frame except at the end of the film or when loading, when the film advance is extended to 125 mm. The problem was that the camera kept defaulting to the extended film advance. After many attempts and communications with the manufacturing company the fault could not be rectified.

Subsequently the flash unit was removed from the vehicle and found to have leaked. Water could be seen in the glass dome housing. The amount of water - a cup full - suggested that this could have been a low pressure leak around the glass dome 'O' seal. The flash unit had been factory sealed.

Due to these problems, no further photography could be carried out. However, the equipment was utilised to provide two high resolution bathymetric surveys using the pressure and altimeter information from the acoustic telemeter (see below). An additional downward pointing 10 kHz acoustic beacon was fixed to the vehicle to supply sub-bottom profiling information. There were no further problems resulting from this exercise.

A replacement camera and flash unit were ordered for the following cruise (CD100).

SHRIMP fault scarp (pinger) survey

(Neil Mitchell, Roger Searle)

Following the failure of the camera system, we modified the SHRIMP payload by removing cameras and flash units and including a downward-pointing 10 kHz pinger within the SHRIMP frame. This package was twice towed at slow speed up a fault scarp that was identified from CD65 TOBI images as having a large talus ramp partially covered with pelagic sediment. The two lines are located in Figure 16. The purpose of this survey was two-fold. First, we intended to obtain a high-resolution bathymetry profile which could be used to compare with the Simrad and TOBI swath bathymetry data. Second, echo character of bottom reflections from the pinger could be used to infer the nature of the bottom type and hence whether there is significant pelagic sediment on the talus ramp.

SHRIMP altitude above seafloor and pressure (depth below sea-level) were encoded by the onboard computer and relayed to the surface acoustically. These signals were continuously printed on an inkjet printer and on a Waverley grey-scale printer, and altitude and pressure-depth were subsequently digitized from the Waverley record. An example plot with digitizing scale is shown in Figure 17. Pressure was converted to depth using the following formula, and combined with vehicle altitude to produce seafloor depth:

$$v = (-0.000022512\, p + 9.72659)\, p / g,$$

where v is vehicle depth below sealevel in meters, p is water pressure in decibar, and g is the acceleration due to gravity. This formula is estimated to have an accuracy of about 1 m. g varies with both water depth and latitude:

$g = 9.780318\ (1 + (0.0052788 + 0.0000236 \sin^2\phi)\sin^2\phi) + 1.092\text{X}10^{-6} p$, where ϕ is latitude. We evaluated this at 29° N using the average water depth of the survey; the error in assuming constant g was estimated to be 1 part in 4000). This gave an average value of 9.7942 m s^{-2} for g.

Positioning of the SHRIMP vehicle along the profile was calculated by means of a "layback" calculation. The length of cable and vehicle depth were used to determine the offset from the ship and this offset was combined with the ship's GPS navigation using the same algorithm that was used to calculate TOBI positions (see above).

Echo-character from the pinger was recorded on the inkjet printer (essentially the same display used for the transmitted data since the pinger frequency was the same as SHRIMP transponder). Further digital copies of the data were taken by using a screen-dump facility on the vehicle-flyer's display and these files were archived by copying them onto two MS-DOS disks

Preliminary comparisons of the seafloor profiles obtained by the SHRIMP, TOBI profiler and EM12 data showed that they are remarkably similar.

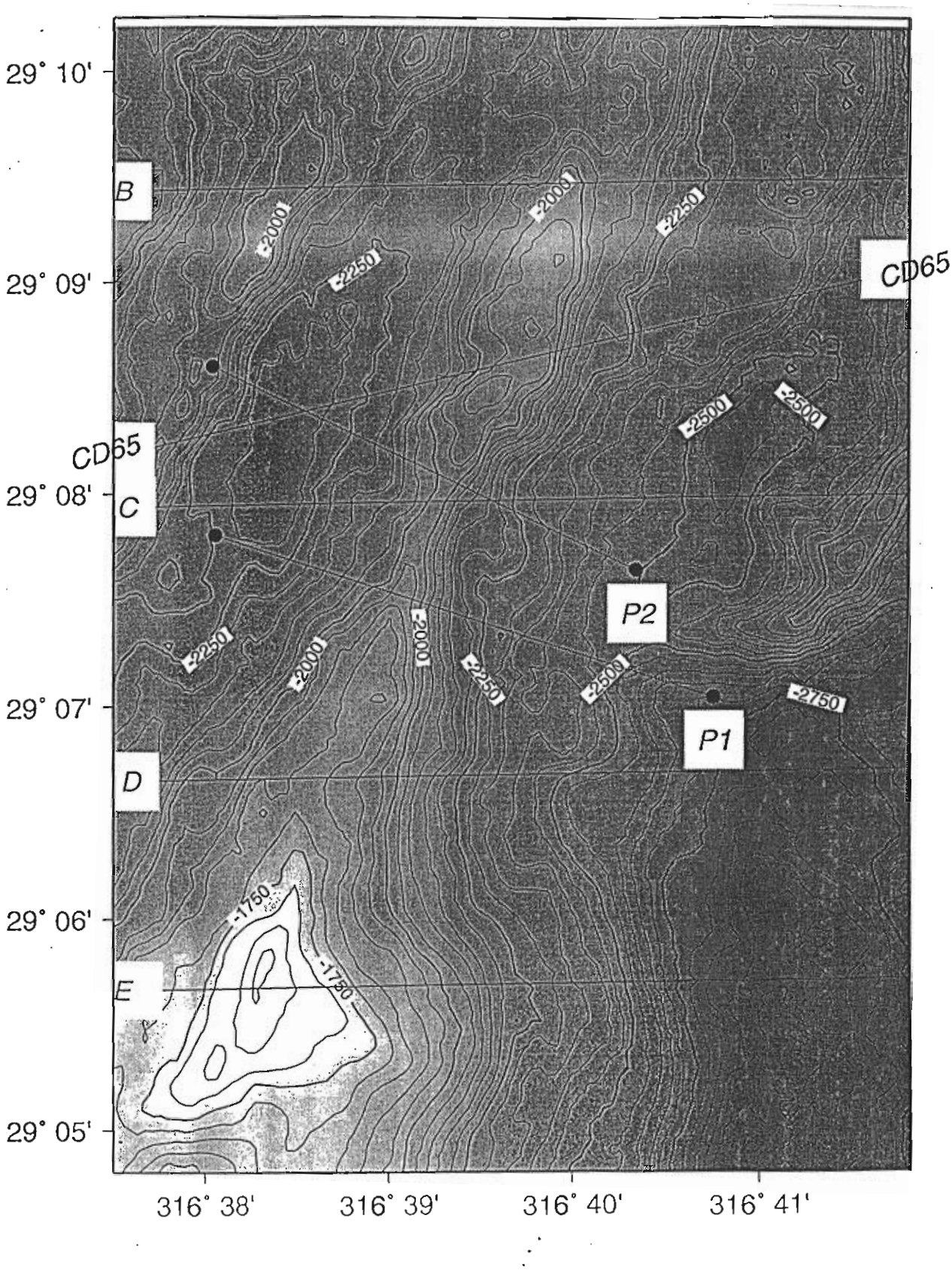

Figure 16: Approximate location of the two SHRIMP pinger survey lines. Line 1 runs from 29.1167N, 43.3200W to 29.1300N, 43.3650W and line 2 runs from 29.1267N, 43.3267W to 29.1433N, 43.3650W.

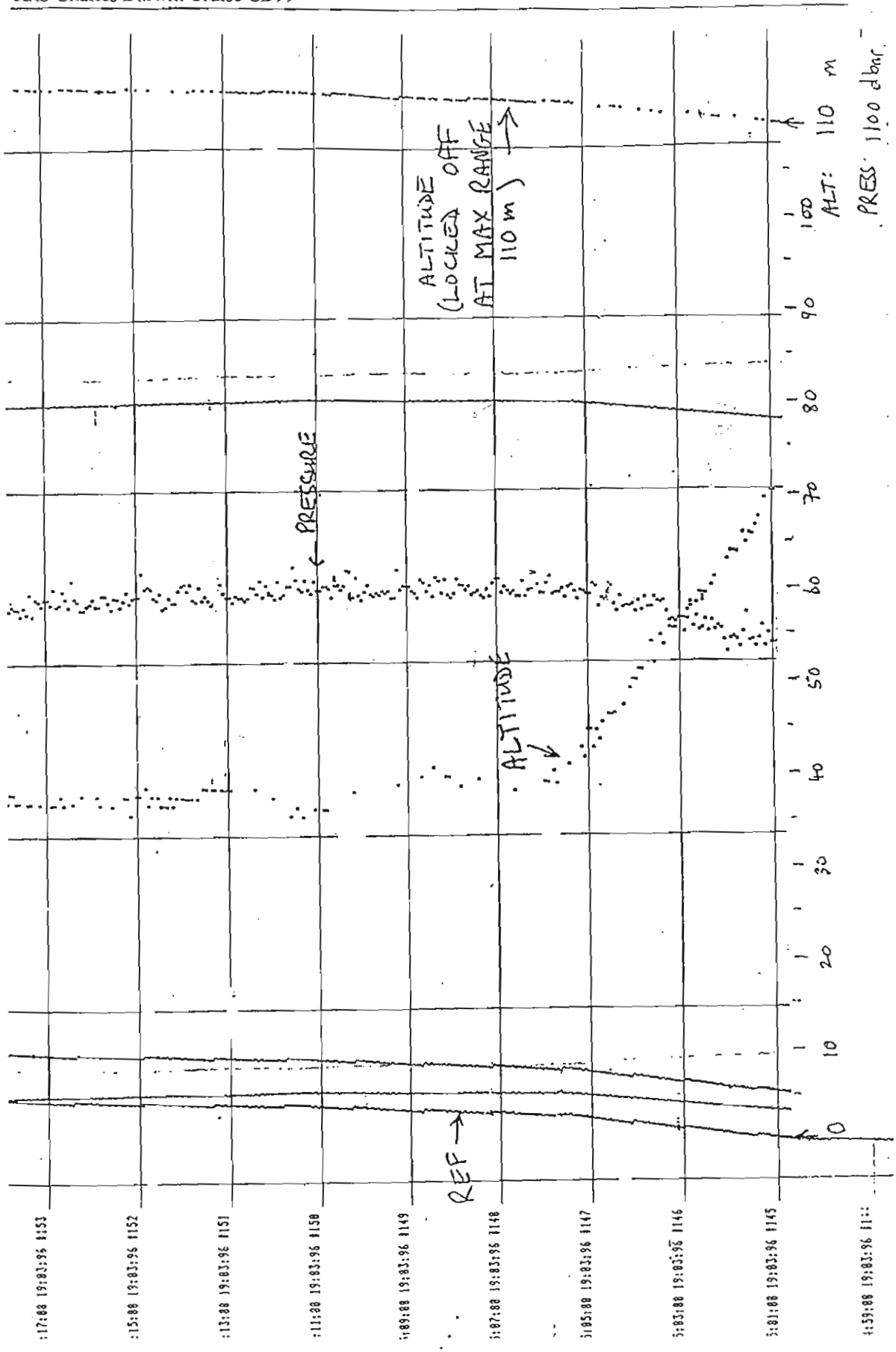

Figure 17: Example Waverley record of fish-flier's display showing how SHRIMP altitude and vehicle depths were digitized. Measurements are made from the 'Ref' trace to the altitude and pressure traces. Scales for vehicle altitude (0 - 110 m) and water pressure at vehicle (0 - 1100 dbar) are shown at the base of the record.

Simrad EM12 data processing

(A. Firn, G. Knight)

The Simrad EM12 multibeam echosounder ran from 060/1600 (200 miles off mainland Portugal) to 098/2339 (en route to Azores) The swath survey conducted on CD99 produced around two gigabytes of raw data . Prior to commencing work in the survey area the instrument was calibrated for drift in the pitch and roll sensor (067/2013-2300): it was found that none had occurred.

The survey requirements of TOBI resulted in a survey plan which gave considerable over-sampling with the EM12 due to the close proximity of the TOBI lines and the slow survey speed. The along-track spacing of returns was typically of the order of twelve metres. This density of along-track data combined with swaths which overlapped by almost a full swath width made possible very fine resolution grids, down to 50 m grid spacing. However, these grids were very much at the limit of resolution of the data as the typical footprint in this area has a width of a hundred metres.

During processing of the sonar returns and in subsequent griding of the data, it was possible to see small system errors. This was particularly apparent when fifty metre grids were made. These errors were of two types. Firstly and most importantly, errors associated with rotational movement of the ship. The ship handling requirements of maintaining the TOBI survey line at speeds of around two knots result in continuous and relatively large heading changes. Particularly when surveying in poor weather these changes in heading exceeded the capability of the pitch roll and heave sensor to compensate fully.

The over sampling of the survey area also resulted in a small amount of noise from the navigation input which was derived from standard GPS. This is hardly unexpected when in some instances data from up to six lines fall within the same fifty metre grid cell. The processed navigation data errors should be considerably less than the one hundred metre worst case specification of the GPS system, but it would be optimistic to think that registration of overlapping swath lines to accuracies of better than thirty metres was achieved.

After careful editing of returns within the Neptune *binstat* statistical editor these problems were minimised in the final data grids produced.

In similar circumstances in the future, the navigation error could be minimised by the use of differential GPS if it were considered necessary. However, the rotational errors make a convincing argument for replacing the present pitch and roll sensor with a more accurate and faster responding measurement system such as an Ashtec GPS.

Sound velocity measurements

(Roger Searle)

Sound velocity and depth/temperature measurements were made throughout the cruise to calibrate the Simrad EM12 echosounder.

We attempted three sound velocity profile measurements: one on 065/0800 (subsequently aborted due to bad weather); one on 067/1500-1800 immediately prior to the EM12 calibration run; and one on 072/0500-0740 on first entering the science work area at Broken Spur. Data from the last of these (Figure 18) were used in the EM12 throughout the rest of the cruise, but were checked by daily XBT deployments.

34 XBTs were deployed while underway, of which the majority were type T5 (1830 m depth capability). Of these, all worked except for TWO partial failures (failed at 300m and 800m depth) and four complete failures. The profiles derived from the XBT stations in the science area were remarkably consistent (Figure 19), not requiring any update of the EM12 calibration.

Finally, the sea surface sound velocity was monitored automatically throughout the cruise. Figure 20 shows the record for one week in the middle of the cruise: rms variation is well within $\pm$ 1 ms^{-1}.

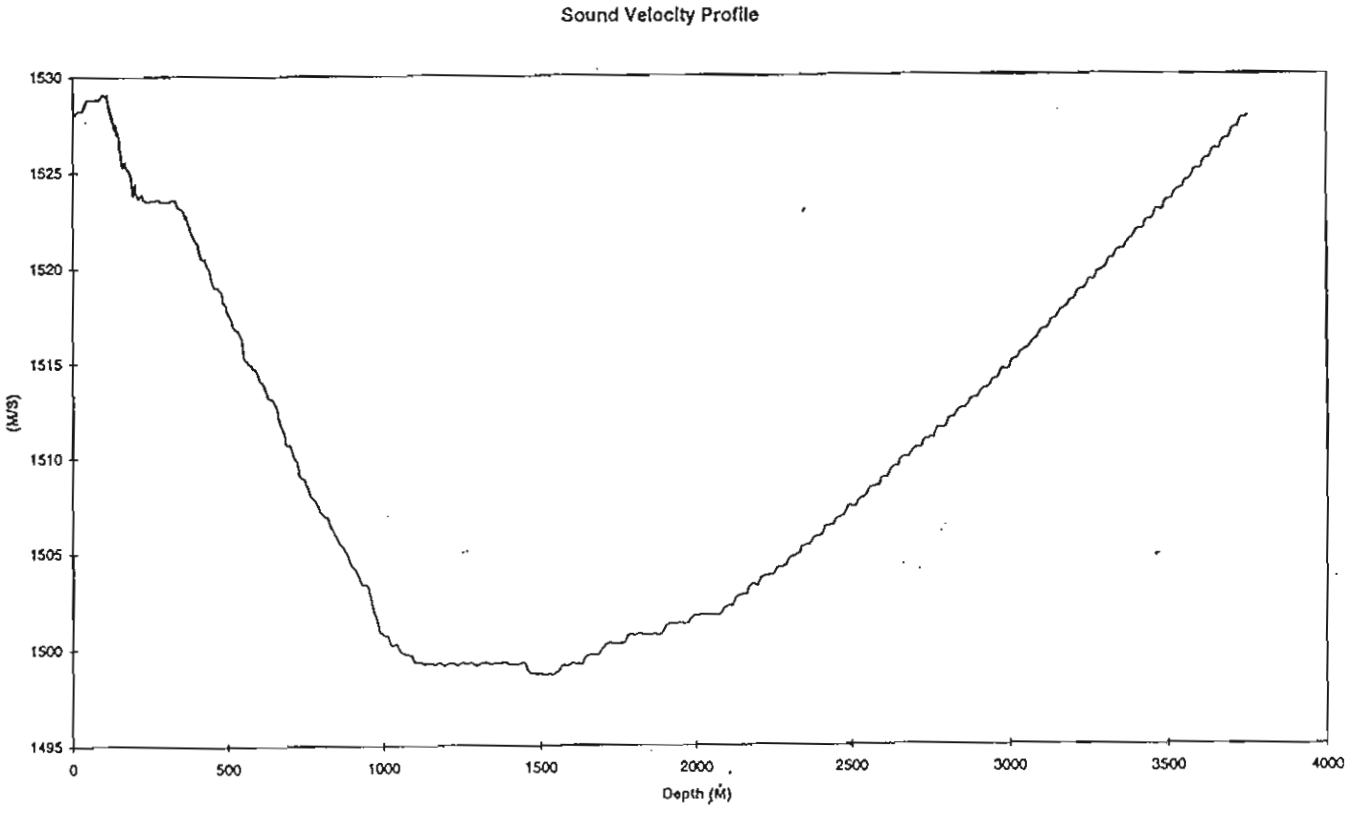

Figure 18: Sound velocity profile from sound velocitymeter station SVP3 (072/0500) used for EM12 calibration for the duration of work in the science area.

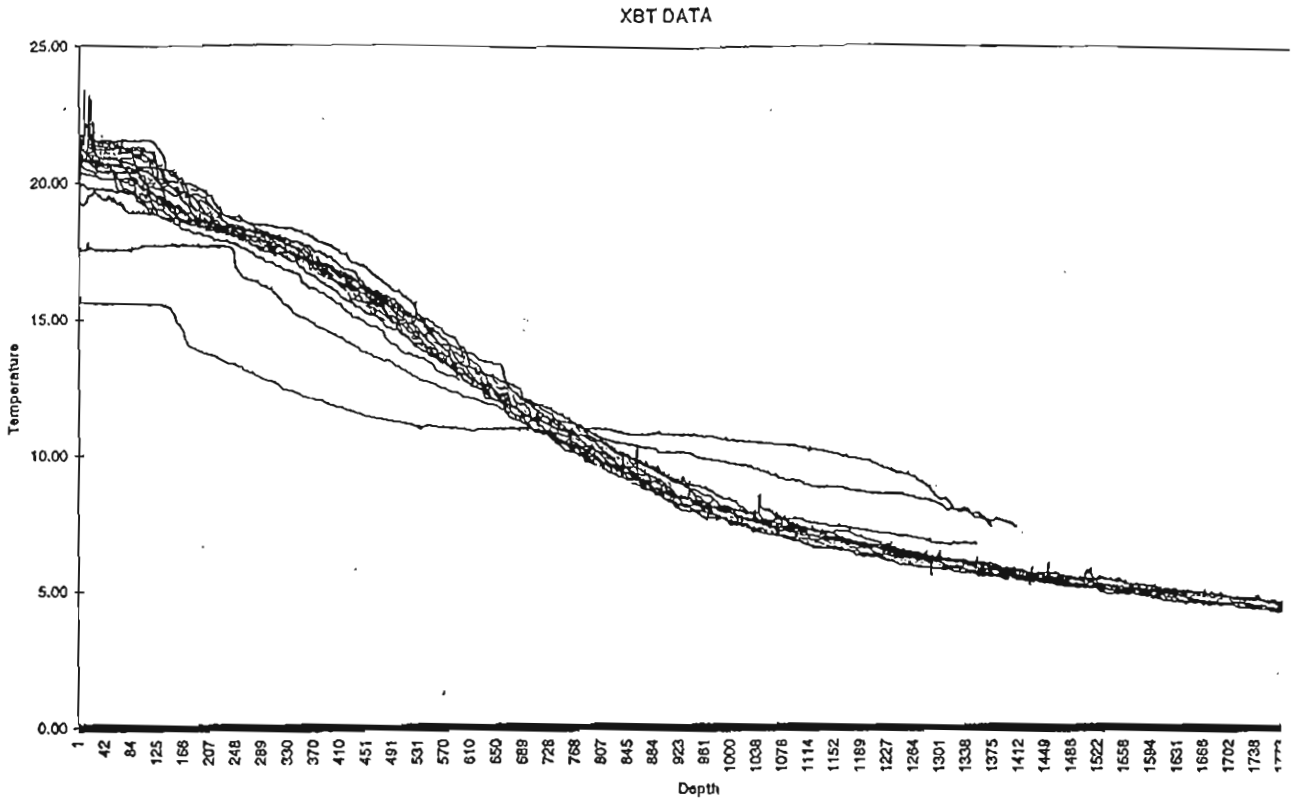

Figure 19: Stacked temperature/depth profiles from the XBT deployments on CD99.

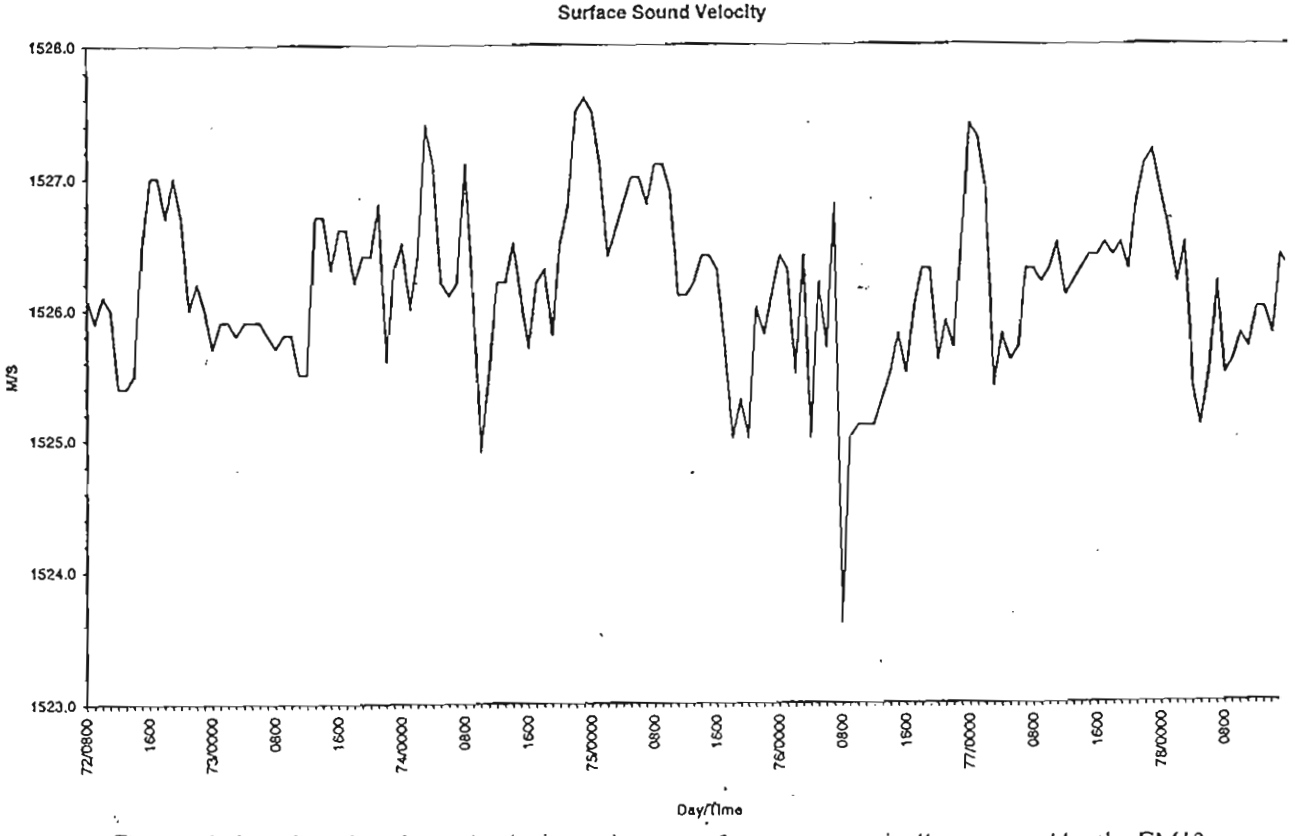

Figure 20: Running plot of sound velocity at the sea surface as automatically measured by the EM12.

Shipboard Computing Network

(G. Knight, A. Firn)

Ship Computing Installation

Navigation, gravity and magnetics data were logged continuously and processed. All parts of the ship's data-collection and data-processing system worked reliably throughout CD99. The final navigation was resolved to a 10s interval, as were processed gravity and magnetics.

Guest machines

A satisfactory network of all UNIX workstations provided for use on CD99 with the existing ship system was configured. The variety of operating systems used, i.e. SunOS, Solaris and Linix, coupled with the working environments that the systems had been configured for initially, made this task less easy than had been anticipated.

RVS Scientific Engineering Group

(Pete Mason, Colin Day)

A replacement conducting cable was installed on the dredge winch for use with TOBI during this and the following cruise. This cable was subsequently deployed to 8,300m and recovered under tension to ensure that the cable was evenly tensioned on the storage drum, this exercise took place whilst on passage to the work area.

At the start of the cruise the CTD winch was used with the starboard gantry to deploy a sound velocity meter.

The trawl winch was used via the starboard gantry to deploy the SHRIMP system and later a pinger system mounted in the SHRIMP cage. These deployments required the package to be flown very close the sea floor and the winch required continuous and accurate control to enable this operation to be successful.

The trawl winch was used via the aft gantry to dredge for rocks at specific locations. These dredge sites were completed with the loss of one dredge.

The dredge winch with the conducting cable on it was used for the majority of the cruise via the aft gantry for the towing of TOBI. The ship's and TOBI's position were continuously plotted by the winch operator during these survey periods.

The starboard aft crane, umbilical winch and the deck mounted three tonne winch were used successfully for the deployment and recovery of the TOBI.

The winch system in one configuration or another was in continuous uses for the majority of the time that the ship was in the work area. All the above items of equipment operated correctly and reliably for the duration of the cruise, the only failure being a ruptured pipe on the crane which took just over one and a half hours to repair.

References

Bullard, E.C. and Mason, R.G. The magnetic field astern of a ship. Deep-Sea Research, Vol. 8, pp 20-27, 1961.

Hussenoeder, S.A., M.A. Tivey, and H. Schouten, 1995, Direct inversion of potential fields from an uneven track with application to the Mid-Atlantic Ridge, Geophysical Research Letters, 22, 3131-3134.

Isezaki, N. A new shipboard three-component magnetometer. Geophysics, Vol. 51, (10), 1992-1998, 1986.

Isezaki, N., J. Matsuda, H. Inokuchi, and K.Yasukawa, shipboad mesurement of three components of geomagnetic field, J.Geomag. Geoelectr., 33, 329-333, 1981.

Nogi, Y., N. Seama, and N. Isezaki, Preliminary report of three components of geomagnetic field measured on board the icebreaker SHIRASE during JARE-30,1988-1989, Proceedings of the NIPR symposiumm on Antarctic Geosciences, 4, 191-200,1990.

Parker, R.L, and S.P. Huestis, 1974, The inversion of magnetic anomalies in the presence of topography, J. Geophys. Res., 79, 1587-1593.

Seama, N., T. Ichikita, and N. Isezaki, Measurement of three component geomagnetic field by STCM, in Preliminary Report of the Hakuho Maru Cruise KH-89-1.J. Segawa Ed., Ocean Res. Inst., University of Tokyo, 50-57, 1990.

Seama, N., and Isezaki, Sea-floor magnetization in the eastern part of the Japan Basin and its tectonic implicaations, Tectonophysics, 181, 285-297,1990.

Seama, N., Y. Nogi, and N. Isezaki, A new method for precise determination of the position and strike of mgnetic boundaries using vector data of the geomagnetic anomaly field, Geophys. J. Int,. 113, 155-164,1993.

Wessel, P., and W.H.F. Smith, Free software helps map and display data, EOS, Transactions of the American Geophysical Union, 72, 441, 445-446, 1991.

Wessel, P., and W.H.F. Smith, New version of the Generic Mapping Tools released, EOS, Transactions of the American Geophysical Union, 76, 329, 1995.

Cruise personnel

Scientific Personnel

Prof. R. C. Searle	University of Durham	Chief Scientist
Dr. N. C. Mitchell	University of Durham	Co-PI
Dr. P. Cowie	University of Edinburgh	Co-PI
Dr. S. Allerton	University of Edinburgh	
Dr. C. J. MacLeod	University of Cardiff	
Dr. J. Escartin	University of Durham	
Dr. P. Slootweg	University of Durham	
Mr. S. Russell	Universities of Durham/Southampton	Student
Ms. Tomoko Tanaka	University of Chiba (Japan)	Guest scientist
Mr. C. Flewellen	Southampton Oceanography Centre	TOBI
Mr. I. Rouse	Southampton Oceanography Centre	TOBI
Mr. D. Edge	Southampton Oceanography Centre	TOBI/SHRIMP
Mr. A. Fern	Research Vessel Services	Computing
Mr. G. Knight	Research Vessel Services	Computing
Mr. P. Mason	Research Vessel Services	Mechanical engineer
Mr. Colin Day	Research Vessel Services	Mechanical engineer
Mr. D. Teare	Research Vessel Services	Instrument engineer
Mr. D. D. Booth	Research Vessel Services	Instrument engineer

Ship's staff

R.A. Bourne	Master
P.W. Newton	Chief Officer
P.T. Oldfield	Second Officer
A.V. MacKay	Third Officer
J.G. Baker	Radio Officer
I.G. McGill	Chief Engineer
J.R. Crosbie	Second Engineer
R.J. Perram	Third Engineer
P.G. Parker	Electrical Engineer
M.J. Drayton	Bosun (CPO deck)
T.G. Lewis	Petty Officer (deck)
P.H. Dean	Seaman
D. Buffery	Seaman
R. Dickinson	Seaman
I.N. Thomsom	Seaman
A.M. Bridge	Motorman
E. Staite	Senior Catering Manager
J.J. Swenson	Chef
R.A. Edes	Master Steward
F. Hardacre	Steward
G.M. Mingay	Steward

Summary of operations with approximate times

See "Diary of events" (page 9) for details

Operation	Start				Duration		End			
	Month	Date	Day	Hour	Days	Hours	Month	Date	Day	Hour
Passage to 200 mile limit	March	3	Sun	19	0	21	March	4	Mon	16
Passage	March	4	Mon	16	0	22	March	5	Tue	14
Tension cable	March	5	Tue	14	0	6	March	5	Tue	20
Passage	March	5	Tue	20	1	19	March	7	Thu	15
Velocimeter station	March	7	Thu	15	0	3	March	7	Thu	18
Simrad calibration	March	7	Thu	18	0	5	March	7	Thu	23
Passage	March	7	Thu	23	0	10	March	8	Fri	09
TOBI test	March	8	Fri	09	0	5	March	8	Fri	14
Passage	March	8	Fri	14	0	23	March	9	Sat	13
TOBI test	March	9	Sat	13	0	20	March	10	Sun	09
Magnetometer calibration	March	10	Sun	09	0	2	March	10	Sun	11
Passage	March	10	Sun	11	1	5	March	11	Mon	16
TOBI test	March	11	Mon	16	0	1	March	11	Mon	17
Passage to science area	March	11	Mon	17	0	12	March	12	Tue	05
Velocimeter station	March	12	Tue	05	0	3	March	12	Tue	08
SHRIMP (abandoned)	March	12	Tue	08	0	2	March	12	Tue	10
STCM calibration	March	12	Tue	10	0	1	March	12	Tue	11
10 kHz line	March	12	Tue	11	0	2	March	12	Tue	13
Dredge D1	March	12	Tue	13	0	4	March	12	Tue	17
TOBI test	March	12	Tue	17	0	10	March	13	Wed	03
SHRIMP	March	13	Wed	03	0	5	March	13	Wed	08
Dredge D2	March	13	Wed	08	0	6	March	13	Wed	14
Dredge D3	March	13	Wed	14	0	5	March	13	Wed	19
EM12 survey	March	13	Wed	19	0	15	March	14	Thu	10
STCM calibration	March	14	Thu	10	0	2	March	14	Thu	12
TOBI line 1 (T)	March	14	Thu	12	0	16	March	15	Fri	04
Wire test SHRIMP	March	15	Fri	04	0	5	March	15	Fri	09
STCM	March	15	Fri	09	0	2	March	15	Fri	11
Dredge D4	March	15	Fri	11	0	5	March	15	Fri	16
Dredge D5	March	15	Fri	16	0	4	March	15	Fri	20
Simrad survey	March	15	Fri	20	0	13	March	16	Sat	09
TOBI line 2 (G)	March	16	Sat	09	1	5	March	17	Sun	14
TOBI line 3 (I)	March	17	Sun	14	1	6	March	18	Mon	20
Pinger P1	March	18	Mon	20	0	7	March	19	Tue	03
Pinger P2	March	19	Tue	03	0	7	March	19	Tue	10
TOBI line O	March	19	Tue	10	1	1	March	20	Wed	11
TOBI line M	March	20	Wed	11	1	5	March	21	Thu	16
TOBI line Q	March	21	Thu	16	0	23	March	22	Fri	15
TOBI line S	March	22	Fri	15	1	15	March	24	Sun	06
Passage	March	24	Sun	06	0	5	March	24	Sun	11
TOBI line K	March	24	Sun	11	0	18	March	25	Mon	05
Passage	March	25	Mon	05	0	5	March	25	Mon	10
TOBI Line E	March	25	Mon	10	1	1	March	26	Tue	11
TOBI line C	March	26	Tue	11	0	24	March	27	Wed	11
TOBI line A	March	27	Wed	11	1	1	March	28	Thu	12
Safety pin turn	March	28	Thu	12	0	4	March	28	Thu	16
TOBI line F	March	28	Thu	16	0	18	March	29	Fri	10
TOBI line J (east)	March	29	Fri	10	0	11	March	29	Fri	21
Dredge D6	March	29	Fri	21	0	6	March	30	Sat	03
Dredge D7	March	30	Sat	03	0	5	March	30	Sat	08
Passage and deployment	March	30	Sat	08	0	4	March	30	Sat	12
TOBI line J (west)	March	30	Sat	12	0	15	March	31	Sun	03
TOBI line H	March	31	Sun	03	0	22	April	1	Mon	01
TOBI line L	April	1	Mon	01	1	0	April	2	Tue	01
TOBI line N	April	2	Tue	01	0	22	April	2	Tue	23
TOBI line P	April	2	Tue	23	0	17	April	3	Wed	16
TOBI line U	April	3	Wed	16	0	12	April	4	Thu	04
TOBI line U-V	April	4	Thu	04	0	4	April	4	Thu	08
TOBI line V	April	4	Thu	08	0	9	April	4	Thu	17
Line R	April	4	Thu	17	0	9	April	5	Fri	02
Recovery	April	5	Fri	02	0	2	April	5	Fri	04
Passage to Ponta Delgada	April	5	Fri	04	4	0	April	9	Tue	04

Tobi bathymetry output types

file	start		end	line(s)[1]	bathy type[3]	duration (min)
t405	140396:1406.80	to	150396:0311.63	T	8	785
t405a	160396:1106.20	to	160396:1118.00	G	8	12
t405b	160396:1433.37	to	160396:1727.60	G	8	174
t406	160396:1727.73	to	170396:0936.87	G	1	969
t407	170396:0936.93	to	180396:0147.67	GtI	8	971
t408	180396:0147.73	to	180396:1756.90	I	1	969
t409	190396:1347.77	to	190396:1920.60	O	2	333
t410	190396:1922.13	to	190396:2205.57	O	2	163
t410a	190396:2207.37	to	200396:0840.80	O	2	633
t410b	200396:1025	to	200396:1102	M	?	37
t410c	200396:1347.83	to	200396:1603.07	M	8	135
t411	200396:1603.13	to	210396:0812.27	M	3	969
t412	210396:0812.33	to	220396:0021.47	MtQ	3	969
t413	220396:0021.53	to	220396:1630.67	QtS	3	966
t413a	220396:1630.73	to	220396:1857.17	S	4	146
t414	220396:1858.77	to	220396:1859.57	S	4	1
t414a	220396:1900.77	to	220396:2359.27	S	4	298
t414b	230396:1222.40	to	230396:2332.07	S	5	670
t415	230396:2332.13	to	240396:0832.30	St	5	540
t415a	240396:1056.17	to	240396:1805.10	K	5	429
t416	240396:1805.23	to	250396:1014.37	Kt	5	969
t417	250396:1014.43	to	260396:0223.57	tE	5	969
t418	260396:0223.63	to	260396:0914.03	Et	5	410
t418a	260396:1500.67	to	270396:0006.53	C	5	546
t419	270396:0006.67	to	270396:1615.83	CtA	5	969
t420	270396:1615.90	to	280396:0825.03	A	5	969
t421	280396:0825.10	to	280396:1524.20	At8	5	419
t421a	280396:1747	to	290396:0258	F	5	551
t422	290396:0258.03	to	290396:0818.10	F	5	320
t422a	290396:0842.63	to	290396:1857.90	tJ	5	615
t423	300396:1245.00	to	310396:0454.13	JtH	6	969
t424	310396:0454.27	to	310396:2103.40	H	6	969
t425	310396:2103.47	to	310396:2355.97	H	7	172
t425a	010496:0352.10	to	010496:1717.33	L	7	805
t426	010496:1717.47	to	010496:2021.43	L	7	184
t426a	020496:0136.97	to	020496:1442.07	tN	7	785
t427	020496:1442.20	to	030496:0504.87	NtP	7	863
t427a	030496:1120.53	to	030496:1306.97	P	7	106
t428	030496:1307.03	to	040496:0516.17	PtUt	7	969
t429	040496:0516.23	to	040496:2125.37	tV	7	969
t430	040496:2125.43	to	050496:0343.60	tR	7	378
t434b	230496:0025.87	to	230496:1343.97	P[2]	7	798
t435	230496:1344.03	to	230496:1853.67	R[2]	7	310

[1] t indicates a turn.

[2] Kindly run for us by Prof. J. R. Cann on CD100.

[3] Bathymetry types:

1: 3850 samples (time 100-3950 ms) of depth below Tobi versus time (starboard only).
Method unknown, but generated in Tobi.
32.3 hours (7.9 %)

2: 2 × 3850 samples of depth below Tobi.
UNAMBiguous phase (of previous ping) is used to steer the AMB reception to avoid ambiguities. Very noisy.
Starboard signal shows some structure, but is unstable.
Port shows 100 % noise. The values are uncorrected m.
18.8 hours (4.5 %).

3: 2 × 3850 samples of depth below Tobi. Same method, but port also shows some structure and the same instability.
48.5 hours (11.7 %).

4: 2 × 3850 samples of AMBiguous phase.
A flat bottom assumption at 200 m was implemented by steering the receiver phase, resulting in less wraps (which in this case could go both up and down).
7.4 hours (1.8 %).

5: 2 × 3850 samples of AMBiguous phase with a flat bottom assumption of 400 m.
139.6 hours (33.8 %).

6: 2 × 1875 samples (time 100-1975 ms) of pure AMBiguous phase (no flat bottom assumed) and
2 × 1975 samples (time probably 0-1975 ms) of UNAMBiguous phase.
32.3 hours (7.9 %).

7: 2 × 987 samples (time 100-1974 ms) of pure AMBiguous phase (each sample alternated with a zero,by accident)
and
2 × 1975 samples (time 100-3950 ms) of UNAMBiguous phase.
A frequency difference between the fm-encoder in TOBI and the shipboard fm-decoder destroys the values of the AMB signal every second. Recuperation is possible after inverse processing of AMB values.
80.8 hours (20.4 %) of CD99 runs only;
99.4 hours (24.1 %) including the two CD100 runs.

8: Not analysed test runs.
34.6 hours (8.3 %).